

**People's Democratic Republic of Algeria
Ministry of Higher Education and Scientific Research**

University M'Hamed BOUGARA – Boumerdes



Institute of Electrical and Electronic Engineering

Department of Electronics

Final Year Project Report Presented in Partial Fulfilment of
the Requirements for the Degree of

MASTER

In Control

Option: Control

Title:

**Study and Simulation of a stand-alone PV
array -battery charging system with MPPT**

Presented by:

- **DOUIFI Nadia**
- **SLIMANI Rania**

Supervisor:

Dr. OUADI Abderrahmane

Co-Supervisor:

Prof. BENTARZI Hamid

Registration Number:...../2020

Abstract

Energy security and independence is one of the most growing concerns around the globe, combined with the environmental impact of traditional energy sources, renewable energy systems have become of great importance. Photovoltaic (PV) systems are the most popular form of renewable energy, as price has become reasonable, and deployment is scalable. However, in many schemes, Photovoltaic systems require rechargeable batteries for energy storage. For Photovoltaic systems, an excessive energy produced by solar cells during intense sunlight peak conditions could damage the batteries. A battery charging controller is therefore used to maintain the suitable charging voltage to the battery so that, as the input voltage from the PV module rises, the charging controller regulates the process, thus, preventing any overcharging. For fast charging, a Maximum Power Point Tracker (MPPT) is used to extract as much power as possible from Photovoltaic modules. In recent years different Maximum Power Point algorithms are developed for Photovoltaic systems to track the changing irradiance and maintain operation point at maximum power. The aim of this thesis is to design and simulate a Photovoltaic system with Maximum Power Point Tracker combined with battery charging controller to charge the battery properly with Constant Current-Constant Voltage (CC-CV) technique and to avoid charging problems. Also a comparison between Perturb and Observe (P&O) and Particle Swarm Optimization (PSO) algorithms is done under uniform and non-uniform solar irradiation to find the MPPT algorithm that converges rapidly and obtain the best efficiency.

Keywords: Photovoltaic system (PV), Maximum Power Point Tracker (MPPT), Perturb and Observe (P&O), Particle Swarm Optimization (PSO), Charging controller, Constant Current-Constant Voltage technique (CC-CV).

Dedication

I dedicate this thesis to my beloved parents, who have been my source of inspiration and gave me strength when I thought of giving up, who continually provide their moral, spiritual, emotional and financial support. Thank you so much for believing in me. You are the best parents in the world, and I owe my success to you.

To my sisters Safia, Amina and Nesrine, my brother Saber and all my nieces and nephews who have never left my side and supported me throughout the process. I will be always grateful to all what they have done.

Furthermore, I dedicate this thesis to my friends especially Amina, Ferial, Rania and Yasmine who made my university experience unforgettable.

Nadia

I have a great pleasure to dedicate this work

To my parents for their endless love, support and encouragement.

To my siblings for giving me strength during my life.

To my grandparents whom I send my greatest love.

To all my teachers who deserve my wholehearted thanks.

To my friends Amina, Ferial, Nadia and Yasmine whom I consider as sisters thank you for the beautiful, crazy and happy moments.

To my soul mate Rania, thank you for being there in times of need.

Rania

Acknowledgment

First of all, we are grateful to almighty ALLAH for giving us strength and ability to understand, learn and complete this project.

*We wish to express our sincere thanks to **Dr.OUADI,Abderrahmane** our thesis supervisor, for his competent guidance and support.*

*We would like also to acknowledge **Prof.BENTARZI,Hamid** for his valuable suggestions and guidance in the preparation of this project.*

We take this opportunity to record our sincere thanks to all IGEE teachers, students, library staff and security service for their valuable help.

We must express our profound gratitude to our parents, family and friends for providing us with unfailing support and continuous encouragement throughout our years of study and through the process of researching and writing this thesis. This accomplishment would not have been possible without them. Thank you.

Finally, we also place on record our sense gratitude to all who directly or indirectly have lent their helping hand in this project.

List of content

| | |
|--|------|
| Abstract..... | I |
| Dedication..... | II |
| Acknowledgment..... | III |
| List of content..... | IV |
| List of tables | VII |
| List of figures | VIII |
| List of Abbreviations | X |
| General introduction..... | 1 |
| Chapter one: Overview of Photovoltaic system. | |
| 1.1. Introduction:..... | 3 |
| 1.2. Photovoltaic physical construction: | 3 |
| 1.2.1. Photovoltaic cell: | 3 |
| 1.2.1.1. Working principle: | 3 |
| 1.2.2. PV module and PV array:..... | 4 |
| 1.3. PV modeling: | 5 |
| 1.4. I-V and P-V characteristics of PV device:..... | 6 |
| 1.4.1. I-V and P-V characteristics of PV cell: | 6 |
| • Solar array parameters: | 7 |
| 1.4.2. I-V characteristics of PV module: | 8 |
| 1.4.2.1. Series combination of PV cells: | 8 |
| 1.4.2.2. Parallel combination of PV cells:..... | 8 |
| 1.4.2.3. Series-Parallel combination of PV cells:..... | 9 |
| 1.4.3. Temperature and irradiance effect on I-V characteristic:..... | 9 |
| 1.4.4. Photovoltaic I-V characteristic with resistive load:..... | 11 |
| 1.5. Partial shading effect: | 12 |
| • Bypass diodes: | 13 |
| • Blocking diodes: | 15 |
| 1.6. Types of PV systems: | 15 |
| 1.6.1. Off-grid “stand alone” PV system:..... | 15 |
| 1.6.2. Grid-tied PV system: | 15 |
| 1.6.3. Interactive PV system:..... | 16 |

| | |
|---|----|
| 1.7. Conclusion: | 17 |
| Chapter two: PV system components and design. | |
| 2.1. Introduction:..... | 18 |
| 2.2. PV system description: | 18 |
| 2.3. Maximum Power Point Tracking: | 19 |
| 2.3.1. DC-DC Converter: | 20 |
| 2.3.2. MPPT algorithms: | 21 |
| 2.3.2.1. Perturb and Observe algorithm: | 22 |
| 2.3.2.2. Particle Swarm Optimization: | 23 |
| 2.4. Storage element: | 25 |
| 2.4.1. Battery types:..... | 25 |
| 2.4.2. Battery specifications: | 26 |
| 2.4.3. Battery technologies: | 27 |
| 2.5. Charging controller:..... | 27 |
| 2.5.1. Boost converter:..... | 28 |
| 2.5.2. Battery charging techniques: | 29 |
| 2.5.2.1. Constant-Current charging (CC):..... | 29 |
| 2.5.2.2. Constant-Voltage charging (CV): | 30 |
| 2.5.2.3. Mixed Constant-Current and Constant-Voltage charging (CC-CV):..... | 30 |
| 2.6. Conclusion: | 32 |
| Chapter three: Simulation and results. | |
| 3.1. Introduction:..... | 33 |
| 3.2. PV array characteristics: | 33 |
| 3.2.1. Under normal conditions: | 33 |
| 3.2.2. Under climate changing conditions: | 35 |
| 3.2.2.1. Irradiance effect: | 35 |
| 3.2.2.2. Temperature effect: | 36 |
| 3.2.3. Under partial shading condition: | 36 |
| 3.3. Maximum Power Point Tracker: | 37 |
| 3.3.1. Perturb and Observe algorithm simulation:..... | 39 |
| 3.3.2. Particle Swarm Optimization simulation: | 42 |
| 3.3.3. Comparison: | 43 |
| 3.4. PV system with battery charging controller: | 43 |

| | |
|--------------------------|----|
| 3.5. Conclusion: | 46 |
| General conclusion | 47 |
| References | |

List of tables

| | |
|--|----|
| Table 3.1: Buck-boost parameters..... | 38 |
| Table 3.2: Initializing P&O parameters..... | 39 |
| Table 3.3: Initializing PSO parameters. | 42 |
| Table 3.4: Comparison of MPPT algorithms. | 43 |
| Table 3.5: Battery characteristics. | 44 |

List of figures

| | |
|--|----|
| Figure 1.1: PV cell working principle. | 4 |
| Figure 1.2: PV cell, module and array..... | 5 |
| Figure 1.3: Single diode equivalent circuit..... | 5 |
| Figure 1.4: I-V and P-V characteristics of a PV cell..... | 7 |
| Figure 1.5: Connection of PV cells in series. | 8 |
| Figure 1.6: Connection of PV cells in parallel. | 9 |
| Figure 1.7: Connection of PV cells in series and parallel. | 9 |
| Figure 1.8: Temperature and irradiance effect on I-V characteristic. | 10 |
| Figure 1.9: Temperature and irradiance effect on P-V characteristic. | 10 |
| Figure 1.10: Location of operating point of PV module. | 11 |
| Figure 1.11: PV system under partial shading..... | 12 |
| Figure 1.12: Bypass and blocking diodes in a PV system..... | 13 |
| Figure 1.13: PV characteristic curves under partial shading with and without bypass diodes. 14 | |
| Figure 1.14: PV characteristic curves for uniform and non-uniform irradiation. | 14 |
| Figure 1.15: Off-grid PV system..... | 15 |
| Figure 1.16: Grid-tied PV system..... | 16 |
| Figure 1.17: Interactive PV system. | 16 |
| Figure 2.1: Block diagram of PV system. | 19 |
| Figure 2.2: MPPT control system..... | 19 |
| Figure 2.3: Non-inverting buck-boost converter. | 20 |
| Figure 2.4: Flowchart of P&O algorithm. | 22 |
| Figure 2.5: P&O schematic diagram. | 23 |
| Figure 2.6: MPPT control based on PSO algorithm..... | 25 |
| Figure 2.7: Boost converter circuit. | 28 |
| Figure 2.8: Constant-Current charging technique. | 29 |
| Figure 2.9: Constant-Voltage charging technique..... | 30 |
| Figure 2.10: CC-CV charging technique..... | 31 |
| Figure 2.11: CC-CV battery charging technique flowchart. | 31 |
| Figure 3.1: PV module specifications. | 33 |
| Figure 3.2: SIMULINK model of single PV module..... | 33 |
| Figure 3.3: I-V and P-V characteristics of single PV module..... | 34 |
| Figure 3.4: SIMULINK model of three PV modules in series under uniform conditions | 34 |

| | |
|--|----|
| Figure 3.5: I-V and P-V characteristics of three PV modules in series..... | 35 |
| Figure 3.6: Irradiance effect on I-V and P-V characteristics curves. | 35 |
| Figure 3.7: Temperature effect on I-V and P-V characteristics curves..... | 36 |
| Figure 3.8: SIMULINK model of three PV modules in series under non-uniform conditions. | 36 |
| Figure 3.9: P-V characteristic curve of PV modules under partial shading. | 37 |
| Figure 3.10: SIMULINK model of PV system with MPPT algorithm. | 37 |
| Figure 3.11: Irradiance and temperature signals. | 38 |
| Figure 3.12: Voltage waveform using P&O under fixed irradiance. | 39 |
| Figure 3.13: Current waveform using P&O under fixed irradiance. | 39 |
| Figure 3.14: Power waveform using P&O under fixed irradiance. | 39 |
| Figure 3.15: Voltage waveform using P&O under varying irradiance. | 40 |
| Figure 3.16: Current waveform using P&O under varying irradiance. | 40 |
| Figure 3.17: Power waveform using P&O under varying irradiance. | 40 |
| Figure 3.18: Voltage waveform using P&O under shaded condition. | 41 |
| Figure 3.19: Current waveform using P&O under shaded condition. | 41 |
| Figure 3.20: Power waveform using P&O under shaded condition. | 41 |
| Figure 3.21: Power waveform using PSO under fixed irradiance. | 42 |
| Figure 3.22: Power waveform using PSO under varying irradiance..... | 42 |
| Figure 3.23: Power waveform using PSO under shaded condition..... | 42 |
| Figure 3.24: SIMULINK model of PV battery charging system with MPPT..... | 43 |
| Figure 3.25: The SIMULINK model of the charging controller..... | 44 |
| Figure 3.26: SIMULINK model of CC-CV controller..... | 44 |
| Figure 3.27: State Of Charge..... | 45 |
| Figure 3.28: Battery charging current. | 45 |
| Figure 3.29: Battery charging voltage. | 45 |

List of Abbreviations

%eff: Percent efficiency
CC: Constant-Current
CC-CV: Constant Current-Constant Voltage
CV: Constant-Voltage
D: Duty cycle
DOD: Depth Of Discharge
FF: Fill Factor
FLC: Fuzzy Logic Control
FOCV: Fractional Open- Circuit Voltage
FSCC: Fractional Short-Circuit Current
 G_{bes} : Global best
GMPP: Global Maximum Power Point
 I_c : Maximum charging current
 I_D : Diode current
 I_{mpp} : Maximum PV output current
INC: Incremental Conductance
 I_{ph} : Photo-current source
 I_{pv} : Photovoltaic current
 I_{SC} : Short-circuit current
li-ion: Lithium-ion
MN: Current source region
MPP: Maximum Power Point
MPPT: Maximum Power Point Tracker
NN: Neural Network
P&O: Perturb and Observe
 P_{besti} : Particle local best
PS: Voltage source region
PSO: Particle Swarm Optimization
PV: Photovoltaic
R: Resistive load
 R_p : Shunt resistance
 R_s : Series resistance

SD: Disconnect signal

SOC: State Of Charge

SoH: State of Health

V_{mpp}: Maximum PV output voltage

V_{OC}: Open-circuit voltage

V_{OCH}: Overcharging voltage

General introduction

General introduction

In the next years, the world is supposed to face several problems related to the exhaustion of some energy sources, mainly those regarding fossil fuels. It is also well known that issues concerned with the increase of oil price due to economic and political matters have been the cause of economic crisis in the last decades. Therefore, the search for renewable energy sources such as wind, solar and ocean becomes more and more intense as a prominent alternative for the mitigation of the world energy crisis.

Photovoltaic power system is considered as the most remarkable energy source among a variety of them because of the characteristic of ecofriendly nature, availability of maintenance and is used in a wide range of fields and various applications such as home electric power supply, military and aerospace parts, battery charging, street light and electric car. However, the efficiency of Solar cell is not only lower than other renewable energy, but also has a problem that the amount of electric power generated by solar arrays changes continuously with weather conditions.

Moreover, the solar cell I-V characteristic is nonlinear and varies with irradiation and temperature. In general, there is a unique point on the I-V or P-V curve, called the Maximum Power Point (MPP), at which the entire PV system operates with maximum efficiency and produces its maximum output power. The location of the MPP is not known, but can be located, either through calculation models or by search algorithms. Therefore, Maximum Power Point Tracking (MPPT) techniques are needed to maintain the PV array's operating point at its MPP.

Partial shading is one of the environmental phenomena that affect the PV arrays and it causes the emergence of multiple peaks in the output power curve and has a huge impact on the efficiency of most of the conventional Maximum Power Point Tracking methods. Thus it is necessary to research MPPT methods that can find the global Maximum Power Point (GMPP) under complex situation.

In PV power generation system, the generated power and the load power requirement are not equal. Hence necessity for storage element "battery" arises. Batteries of PV system are subjected to frequent charging and discharging process. Therefore, charging controller is needed to extend significantly the performance and life of the batteries.

The purpose of this project is to design a PV system with MPPT controller that tracks the Maximum Power Point of the PV array and a battery charging controller that charges the battery safely in short time.

This report is divided into three chapters; the first chapter presents an overview of the Photovoltaic background. The second chapter describes the proposed PV system, after that it provides a review of the literature on the Maximum Power Point Tracking algorithms or methods (P&O and PSO) along with their functionalities, next battery charging controller is presented and different charging techniques are briefly explained. Chapter three presents the MATLAB/SIMULINK implementation of the PV system, it also discusses and compares the MATLAB results for the proposed Maximum Power Point Tracking algorithms and shows the behaviour and performance of each method in terms of time convergence and available power under similar conditions of temperature and irradiation. At the end of this chapter a battery charging controller with Constant Current-Constant Voltage technique is simulated and tested. Finally, a conclusion of the thesis is presented. Moreover, potential research ideas for future work in this field are proposed.

Chapter one:

Overview of Photovoltaic system

1.1.Introduction:

PV systems usage is properly-identified and wide applied in power technologies. Several implementations about to the current technology are evolved. The modelling and simulation of Photovoltaic have made a great transition and form an important part of power generation in this present age. The modelling of PV module generally involves the approximation of the non-linear (I-V/P-V) curves.

The overall performance of Photovoltaic is often stricken by radiation, module temperature and array configurations which have a significant contribution to the reduction of output power. The understanding of the shading impacts and their courting among the output power of the PV array may be also very essential in an effort to find a well overall performance of the PV system.

1.2.Photovoltaic physical construction:

Solar cells are the fundamental devices of a PV system, so to understand the working principle of Photovoltaic system it is necessary to understand the basic operation and the structure of solar cells.

1.2.1.Photovoltaic cell:

PV cell is a device which converts the light energy into electrical energy when light is allowed to fall on this cell. The cell is designed that a large area is exposed to light which enhances the voltage generation across the two terminals of the cell. It is essentially consisting of a semiconductor p-n junction diode with a glass window on top surface layer of p-type. The p-type material is made extremely thin so that incident light photons may easily reach the p-n junction.

Silicon and Germanium are the widely used semiconductor materials for solar cells although gallium arsenide, indium arsenide and cadmium arsenide are also being used nowadays [1].

1.2.1.1. Working principle:

Solar cell or Photovoltaic cell shown in figure 1.1 works on the principle of Photovoltaic effect.

In Photovoltaic effect when light reaches the p-n junction, the light photons can easily enter in the junction, through very thin p-type layer. The light energy, in the form of photons, supplies sufficient energy to the junction to create a number of electron-hole pairs. The incident light breaks the thermal equilibrium condition of the junction. The free electrons in the depletion region can quickly come to the n-type side of the junction. Similarly, the holes in the depletion can quickly come to the p-type side of the junction. Once, the newly created free electrons come to the n-type side, cannot further cross the junction because of barrier potential of the junction. Similarly, the newly created holes once come to the p-type side cannot further cross the junction because of same barrier potential of the junction.

As the concentration of electrons becomes higher in one side “n-type side” and concentration of holes becomes more in another side “the p-type side”, the p-n junction will behave like a small battery cell. A voltage is set up which is known as photo current. If we connect a small load across the junction, there will be a tiny current flowing through it [2].

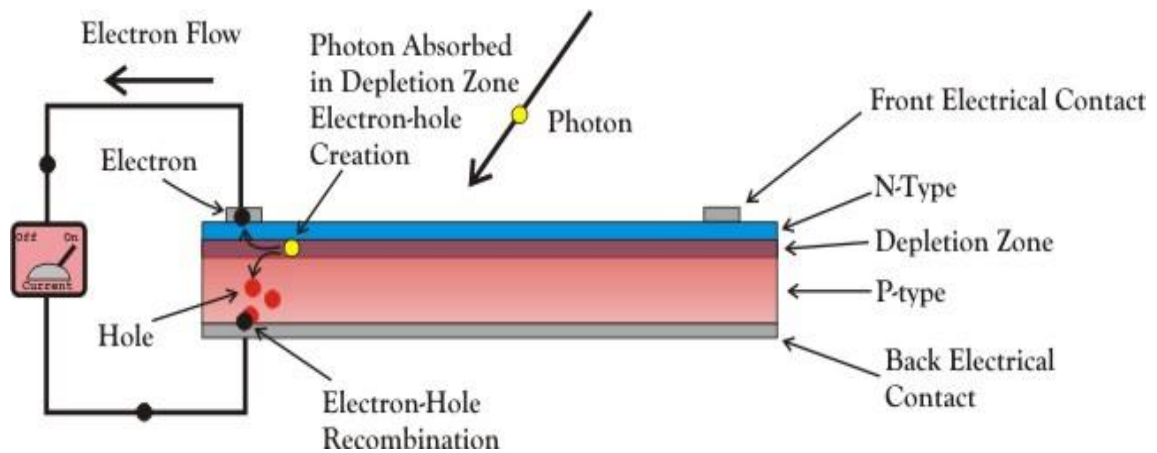


Figure 1.1: PV cell working principle. [2]

1.2.2.PV module and PV array:

A number of individual PV cells are interconnected together (series/parallel) in a sealed, weather proof package called a Panel (Module) to increase their utility. To achieve the desired voltage and current, Modules are wired in series and parallel into what is called a PV Array. The flexibility of the modular PV system allows designers to create solar power systems that can meet a wide variety of electrical needs.

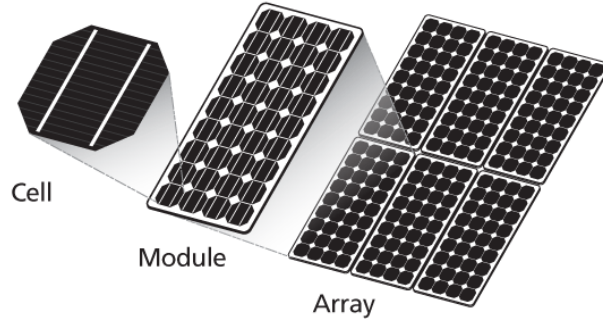


Figure 1.2: PV cell, module and array. [3]

1.3.PV modeling:

In order to predict the power extracted from the solar modules and to plot current-voltage (I-V) characteristics curve, it is important to model the solar cell. The single-diode model shown in figure 1.3 is one of the most commonly-used models; it consists of photo-current source I_{ph} , diode, series of resistor R_s ($R_s=0$ in ideal case) and shunt resistor R_p ($R_p= \infty$ in ideal case).

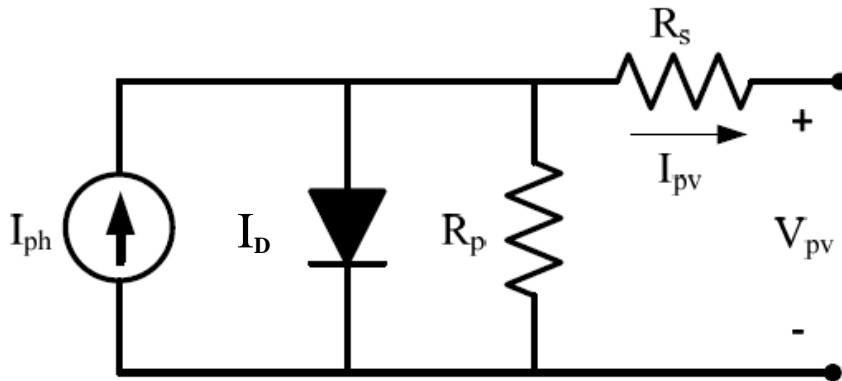


Figure 1.3: Single diode equivalent circuit. [4]

By applying the Kirchoff law to the node of the circuit, the Photovoltaic current I_{pv} produced by the module is obtained as:

$$I_{pv} = I_{ph} - I_D - \frac{V_{pv} + I_{pv}R_s}{R_p} \quad (1.1)$$

The I_D diode current is given by the Shockley equation [5]:

$$I_D = I_0 \left[\exp\left(q \frac{V_{pv} + I_{pv}R_s}{\gamma K T_c}\right) - 1 \right] \quad (1.2)$$

Where:

V_{pv} : the output voltage (V).

I_0 : the saturation diode current (A).

γ : the form factor which represents an index of the cell failing.

T_c : the module temperature (K).

q : the electric charge ($1.602 \times 10^{-19}C$).

K : the Boltzmann's constant ($1.381 \times 10^{-23}K$).

By substituting (1.2) in (1.1), the following equation is obtained as [5]:

$$I_{pv} = I_{ph} - I_0 \left[\exp \left(q \frac{V_{pv} + I_{pv}R_s}{\gamma K T_c} \right) - 1 \right] - \frac{V_{pv} + I_{pv}R_s}{R_p} \quad (1.3)$$

Equation (1.3) represents the I-V characteristic curve equation of a solar cell.

Since the output voltage and current obtained from the single unit of the cell is very small, a PV module is used instead of it.

The output current-voltage characteristic of a PV panel is expressed by equation (1.4), where n_p and n_s are the number of solar cells in parallel and series respectively.

$$I_{pv} = n_p \left[I_{ph} - I_0 \left[\exp \left(q \frac{V_{pv} + I_{pv}R_s}{\gamma K T_c n_s} \right) - 1 \right] - \frac{V_{pv} + I_{pv}R_s n_s}{R_p n_s} \right] \quad (1.4)$$

1.4.I-V and P-V characteristics of PV device:

Equation (1.4) shows that the relation between output voltage and current of PV panels is not linear. The output voltage and current of PV panels are dependent on solar irradiation and ambient temperature, which are naturally variable.

1.4.1.I-V and P-V characteristics of PV cell:

Figure 1.4 shows the I-V and P-V characteristics of a typical silicon PV cell operating under normal conditions.

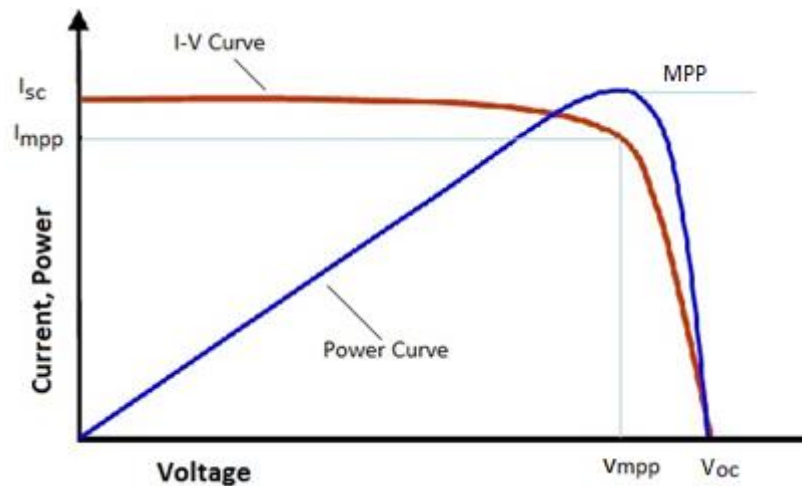


Figure 1.4: I-V and P-V characteristics of a PV cell. [6]

- **Solar array parameters:**

-Open-circuit voltage (V_{OC}): It is the maximum voltage that the array provides when the terminals are not connected to any load (an open circuit condition). This value is much higher than maximum PV output voltage (V_{mpp}) which relates to the operation of the PV array which is fixed by the load. This value depends upon the number of PV panels connected together in series.

-Short-circuit current (I_{SC}): The maximum current provided by the PV array when the output connectors are shorted together (a short circuit condition). This value is much higher than maximum PV output current (I_{mpp}) which relates to the normal operating circuit current.

-Maximum Power Point (MPP): This relates to the point where the power supplied by the array that is connected to the load (batteries, inverters) is at its maximum value. The Maximum Power Point of a Photovoltaic array is measured in Watts (W) or peak Watts (W_p).

-Fill Factor (FF): It is the relationship between the maximum power that the array can actually provide under normal operating conditions and the product of the open-circuit voltage times the short-circuit current, ($V_{OC} * I_{SC}$) This Fill Factor value gives an idea of the quality of the array and the closer the Fill Factor is to 1 (unity), the more power the array can provide. Typical values are between 0.7 and 0.8.

-Percent efficiency (%eff): The efficiency of a Photovoltaic array is the ratio between the maximum electrical power that the array can produce compared to the amount of solar irradiance hitting the array. The efficiency of a typical solar array is normally low at around 10-12% depending on the type of cells (monocrystalline, polycrystalline, amorphous or thin film) being used [7].

1.4.2.I-V characteristics of PV module:

As it is mentioned before, in order to increase the output efficiency a different combination of cells is used. There are three possible ways of combining the PV cells.

1.4.2.1. Series combination of PV cells:

If more than two cells are connected in series with each other, then the output current of the module remains same, and its voltage becomes double (See figure 1.5).

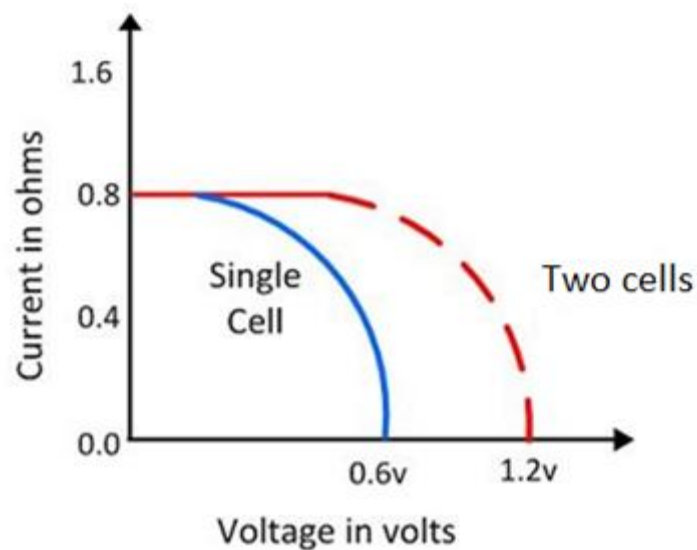


Figure 1.5: Connection of PV cells in series. [8]

1.4.2.2. Parallel combination of PV cells:

In the parallel combination of the cells, the voltage remains same, and the magnitude of current becomes double (See figure 1.6).

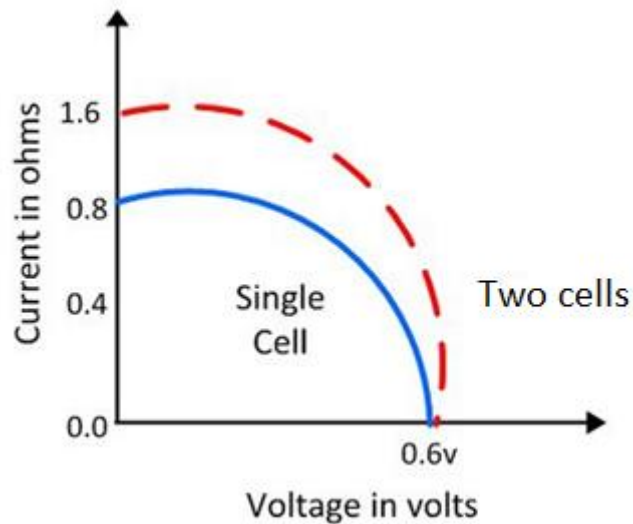


Figure 1.6: Connection of PV cells in parallel. [8]

1.4.2.3. Series-Parallel combination of PV cells:

In the series-parallel combination of cells the magnitude of both voltage and current increases. (See figure 1.7). Thereby, the solar panels are made by using the series-parallel combination of the cells [8].

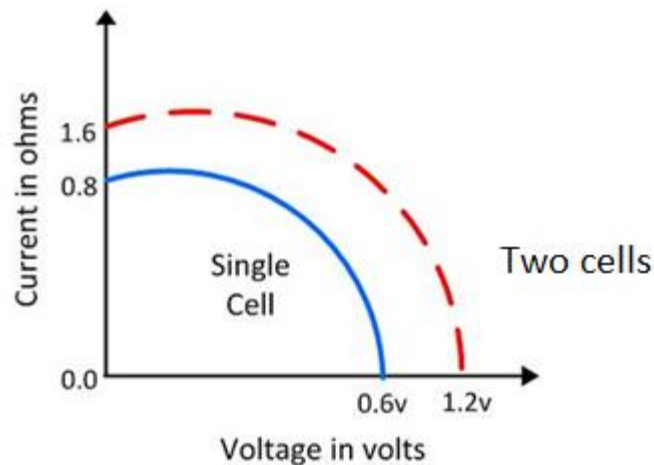


Figure 1.7: Connection of PV cells in series and parallel. [8]

1.4.3. Temperature and irradiance effect on I-V characteristic:

There are various ambient conditions that affect the output of a PV power system. These factors should be taken into consideration. Temperature and irradiance are parameters that have great influence on the behaviour of a PV system, as they modify system efficiency and output energy.

It is evident that the temperature has a significant effect on the open-circuit voltage value, while it has a negligible effect on short-circuit current value. On the other hand, the irradiance value has a direct effect on the short-circuit current of the cell while negligible effect on the open circuit voltage value.

Figure 1.8 and 1.9 shows the effect of temperature and irradiance on I-V and P-V characteristic.

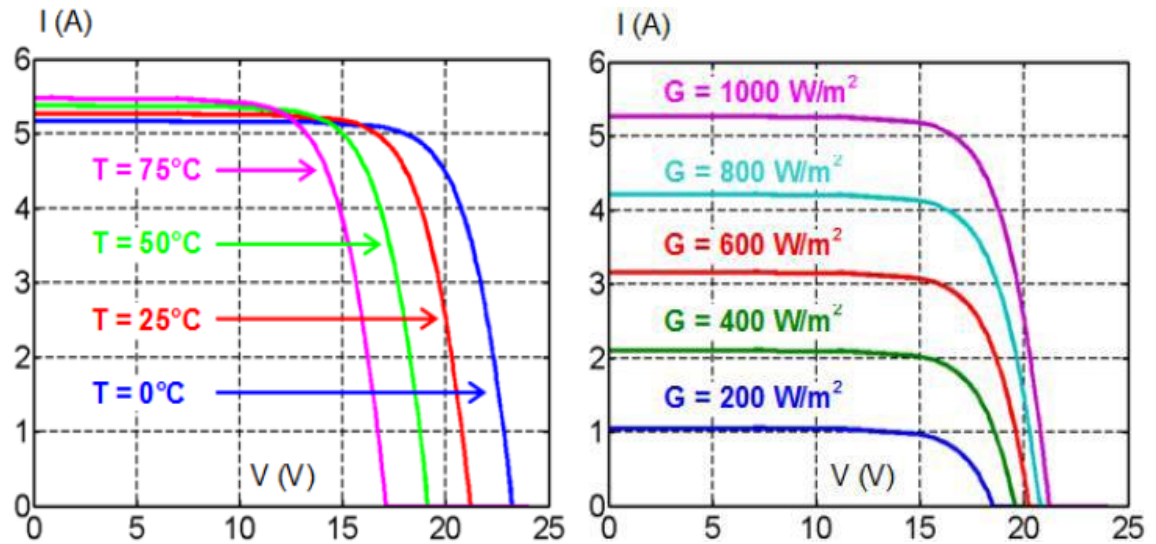


Figure 1.8: Temperature and irradiance effect on I-V characteristic. [9]

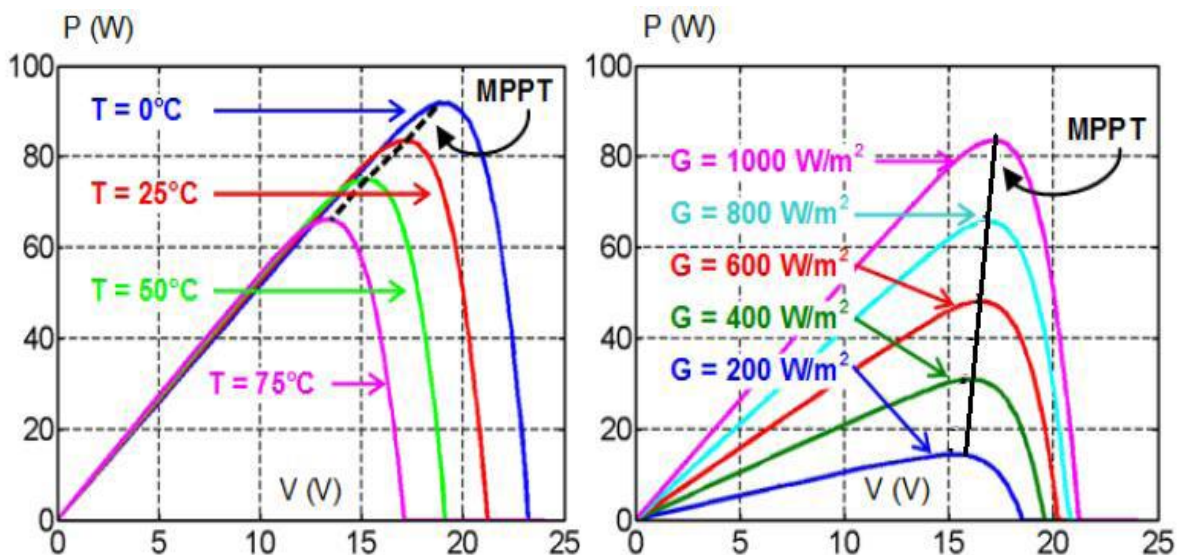


Figure 1.9: Temperature and irradiance effect on P-V characteristic. [9]

From figure 1.8 it is observed that with the increase in temperature the voltage decreases and with the increase in solar irradiance the current increases. And from figure 1.9 it is clear that the output power of PV's is directly proportional with the amount of solar irradiance falling on it, and inversely proportional with its temperature. It also shows that the Maximum Power Point changes with the change of temperature and solar irradiance [4].

1.4.4. Photovoltaic I-V characteristic with resistive load:

The operating characteristic of a PV module consists of two main regions; the voltage source region and current source region. The voltage source region is located at the right of the I-V curve and the internal impedance of the solar module in this region is low. Where the current source region is located on the left of the I-V curve and the internal impedance in this region is high.

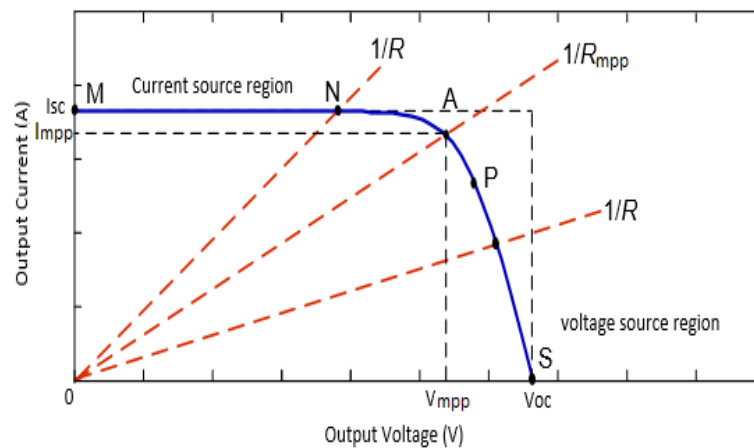


Figure 1.10: Location of operating point of PV module. [10]

When a fixed resistive load (R) is connected directly to the PV module's terminals, the operating point is determined by the intersection of the solar module I-V characteristic with the I-V characteristic of the load. As shown in figure 1.10 the characteristic of the resistive load is a straight line with a slope, $I/V = 1/R$. Additionally, the power delivered to the load depends only on the resistance value. If the load resistance is small, the module operates in the current source region (MN) of the curve, almost near to the short circuit current. Alternatively, if the load resistance is large, the module operates on the voltage source region (PS) of the curve, almost near to the open circuit voltage. If the load line crosses the point A which is the Maximum Power Point

(MPP), then the maximum power can be transferred to this load [10]. The value of this load resistant would be given by [11]:

$$R_{MPP} = \frac{V_{MPP}}{I_{MPP}} \quad (1.5)$$

1.5. Partial shading effect:

Because of large surface that PV system covers, PV modules are not always viable to have steady lighting whole of the time and they can have different irradiance level as a result of shadows caused by trees, high buildings, weather change, presence of clouds and every day sun angle changing.

Figure 1.11 shows PV system under partial shading caused by trees.



Figure 1.11: PV system under partial shading. [12]

In a PV module the shading does not decrease the power only however it leads into current mismatch within a PV series string and voltage mismatch among parallel strings.

A cell can be treated as a combination of a current generator connected with a diode. The photo-current flows in the invert leading of the diode, which means that if one cell is partially shaded, it will product minimal current than the other cells in the string, and the else cells will seek to supply extra current during the bad cell than the poor cell deliver. However, this is not possible ago then the cell works as a diode in the invert trend. Then the current produced in the poor cell will border the current in the string [12]. The shaded cells then operate with a reverse bias voltage to provide the same current as the remaining cells. However, the resulting reverse power polarity leads to

power consumption and a reduction in the maximum output power of the partially-shaded PV module which causes a hot spot to appear on them and creating an open circuit in the entire PV module. In order to avoid power damage and hot spot trouble in the panel during the partial shading a bypass diode is connected in parallel with each PV module [13].

- **Bypass diodes:**

Bypass diodes are quite similar to the diodes that are used in the solar cells where the bypass diodes allow greater amount of current to pass through them with a very little amount of losses in them. In general, as it is shown in figure 1.12 bypass diodes are arranged in reverse bias between the positive and negative output terminals of the solar module and have no effect on its output [14].

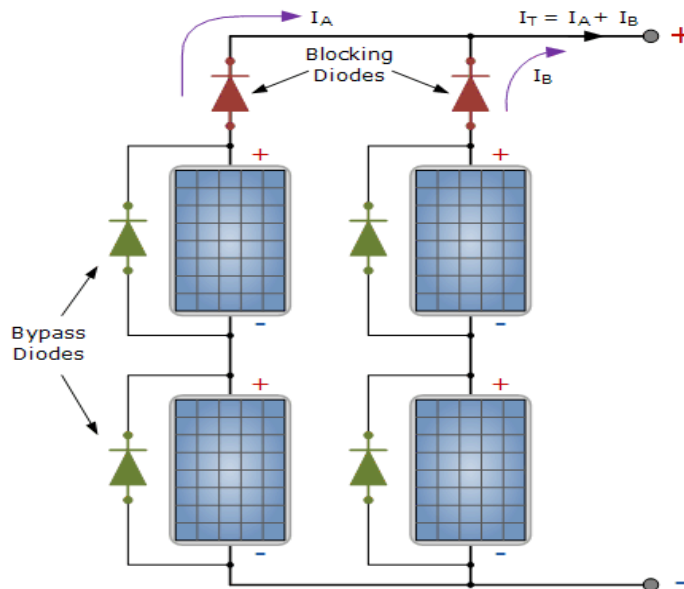


Figure 1.12: Bypass and blocking diodes in a PV system. [14]

Under normal operation, the bypass diode will be reverse biased and will effectively be an open circuit. However, when the module is partially shaded the solar cells are reverse biased due to a mismatch in short-circuit current between several series connected cells, then the bypass diode conducts, thereby allowing the current from the good solar modules to flow in the external circuit rather than forward biasing each good cell. The maximum reverse bias across the poor cell is reduced to about a single diode drop, thus limiting the current and preventing hot-spot heating and ensures the efficiency of the PV system.

From figure 1.13 it can be seen that the characteristics of an array with bypass diodes differ from the one without these diodes. Since the bypass diodes provide an alternate current path, cells of a module no longer carry the same current when they are partially shaded. Therefore, as it is shown in figure 1.14 the power-voltage curve develops multiple maxima (global maxima which is the true MPP while others are local peaks). Unfortunately presenting multiple maxima in the P-V characteristic is a crucial issue and most of the conventional MPPT algorithms may not distinguish between the local and global maxima [13].

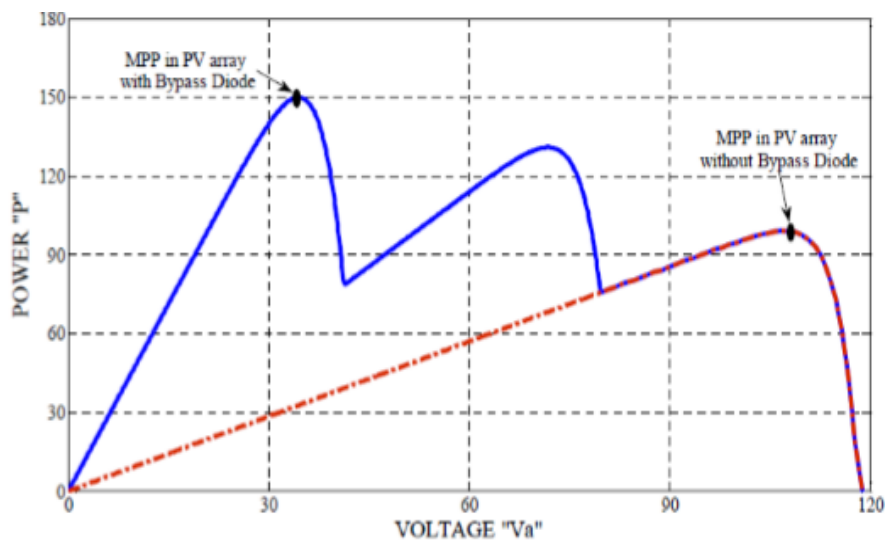


Figure 1.13: PV characteristic curves under partial shading with and without bypass diodes. [13]

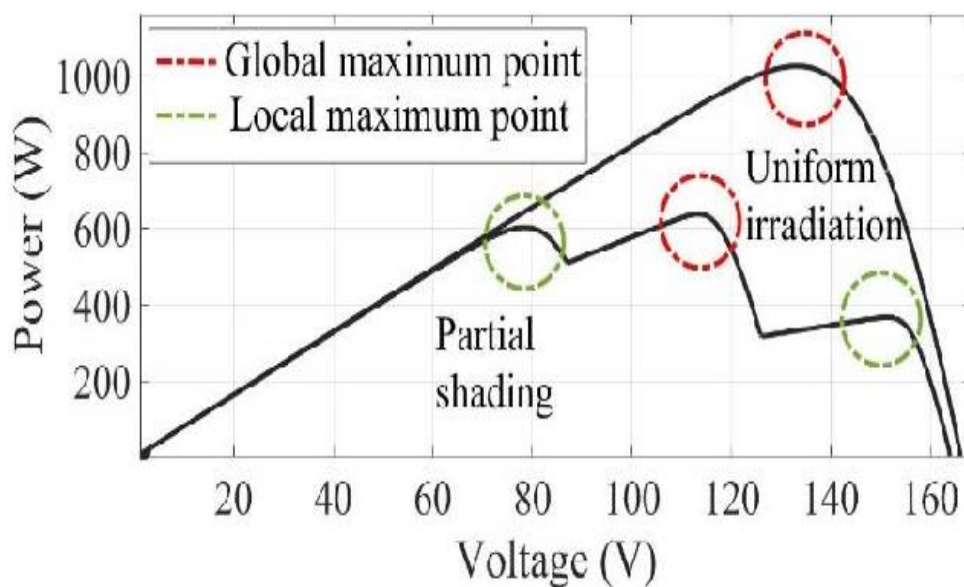


Figure 1.14: PV characteristic curves for uniform and non-uniform irradiation. [15]

- **Blocking diodes:**

Blocking diodes shown in figure 1.12 are used to prevent the batteries from being discharged through the PV cells at night when there is no sun available to generate energy. These blocking diodes also protect the battery from short circuits. In a solar power system consisting of more than one string connected in parallel, if a short circuit occurs in one of the strings, the blocking diode prevents the other PV strings to discharge through the short circuited string [14].

1.6.Types of PV systems:

Photovoltaic power systems are generally classified according to their functional and operational requirements, their component configurations, and how the equipment is connected to other power sources and electrical loads. The principal classifications are:

1.6.1.Off-grid “stand alone” PV system:

An off-grid system (Figure 1.15) is not connected to the electricity grid and therefore it may need battery storage. Off-grid solar systems must be designed appropriately so that they will generate enough power throughout the year and have enough battery capacity to meet the home’s requirements, even in the depths of winter when there is generally much less sunlight. They are usually only needed in more remote areas that are far from the electricity grid [16].

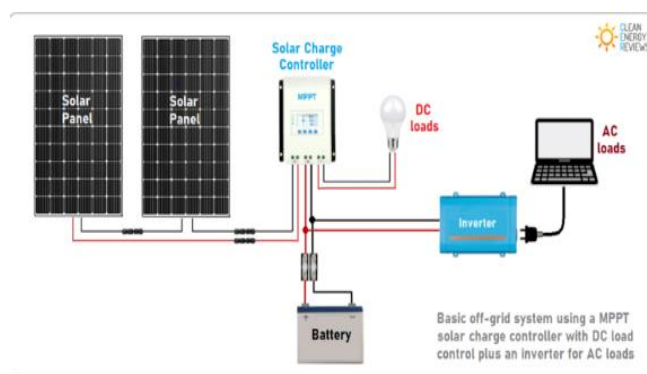


Figure 1.15: Off-grid PV system. [16]

1.6.2.Grid-tied PV system:

On-grid or grid-tie solar systems (Figure 1.16) are by far the most common and widely used by homes and businesses. These systems do not need batteries and use

common solar inverters and are connected to the public electricity grid. Any excess solar power that is generated is exported to the electricity grid.

On-grid solar systems are not able to function or generate electricity during a blackout due to safety reasons. Since blackouts usually occur when the electricity grid is damaged; if the solar inverter was still feeding electricity into a damaged grid it would risk the safety of the people repairing the faults in the network [16].

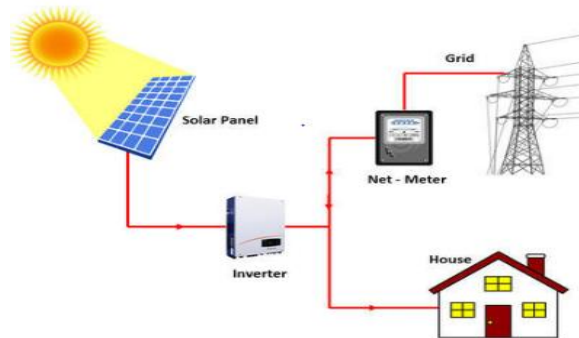


Figure 1.16: Grid-tied PV system. [16]

1.6.3. Interactive PV system:

Modern interactive systems (Figure 1.17) combine solar and battery storage in one and are now available in many different forms and configurations. Due to the decreasing cost of battery storage, systems that are already connected to the electricity grid can start taking advantage of battery storage as well. This means being able to store solar energy that is generated during the day and using it at night. When the stored energy is depleted, the grid is there as a back-up, allowing consumers to have the best of both worlds. Interactive systems are also able to charge the batteries using cheap off-peak electricity. Most interactive solar systems with battery storage are able to automatically isolate from the grid (known as islanding) and continue to supply some power during a blackout [16].



Figure 1.17: Interactive PV system. [16]

1.7.Conclusion:

In this chapter Photovoltaic system which is one of the most dynamically growing energy technologies in the world today was introduced. Besides, working principle and mathematical model of PV cells were presented and explained. Furthermore, the problem of partial shading and climate changing were presented and their effect on the PV array's I-V and P-V characteristics curves was discussed as well.

Chapter two:

PV system components and
design

2.1.Introduction:

While the Photovoltaic panels may seem like a good source of electricity, they have two major problems of low efficiency and intermittency. Their efficiency of converting sun light into electric power is generally small, and the generated electric power changes with weather conditions. Moreover, PV cell characteristics (I-V or V-P) are nonlinear and change with insolation and temperature. To improve the efficiency, it is desirable to operate the PV module at peak power point to deliver maximum power.

In solar PV systems, the PV modules and batteries are the most expensive components. When the batteries are directly connected to the PV modules, there is no protection against overcharging and consequently, battery life-span decreases. To protect batteries from overcharging, charge controller can be used.

In this chapter a PV system will be designed to abstract maximum power from solar modules using different MPPT algorithms and efficiently charge battery with lesser charging time.

2.2.PV system description:

The Photovoltaic system consists of interconnected components designed in a way to achieve the specific target of delivering the desired electricity from a PV panel to the battery. The major components of the designed PV system are Maximum Power Point Tracker, charging controller and storage element (see figure 2.1).

Maximum Power Point Tracker is included in the system to achieve high efficiency system performance and to increase the amount of energy extracted from the PV array which decrease the charging time to the half. It consists of a switch-mode power-converter inserted between the PV source and the load, and the duty ratio of the converter is controlled by a control algorithm to enable tracking of the MPP.

Charging controller is used to charge the batteries safely following the proper charge procedure, it regulates the voltage and current coming from the solar panels going to the battery. Also, it protects the battery from overcharging.

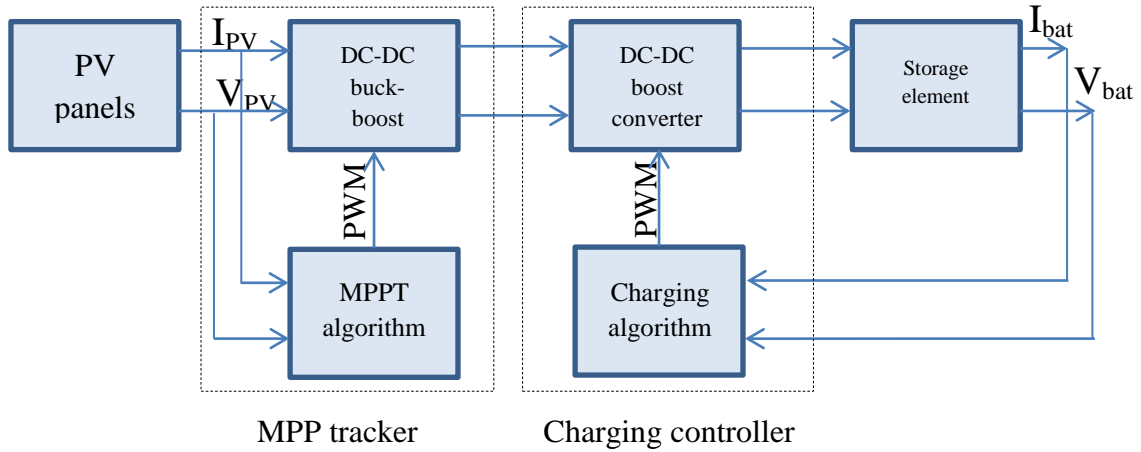


Figure 2.1: Block diagram of PV system.

2.3. Maximum Power Point Tracking:

The productivity of PV systems depends on the variables climatic conditions. So this is why the Maximum Power Point Tracking system control becomes an integral solution to maintain the maximum power production. The MPPT system is basically inserted between the PV array and the load. As illustrated in figure 2.2 the MPPT system consists of two essential components, a DC/DC switching power converter along with an MPPT control algorithm.

In order to efficiently track the MPP, the converter needs to adjust the Duty cycle under varying operating atmospheric conditions in order to match the PV array internal impedance and the output impedance and transfer maximum power to the load. The MPPT controller acquires the real-time operating parameters depending on the control algorithm, and then outputs the corresponding control signal to control the DC/DC buck boost converter [17, 18, and 19].

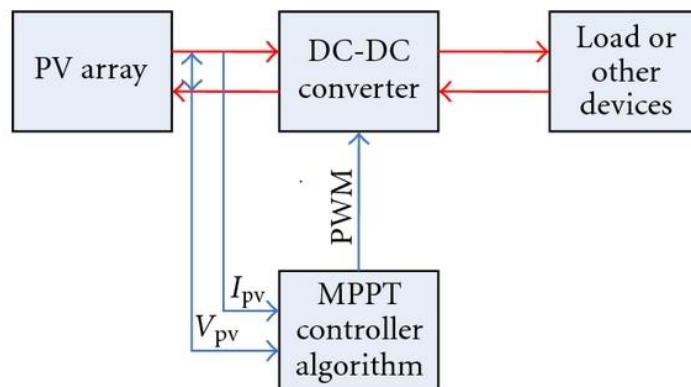


Figure 2.2: MPPT control system. [20]

2.3.1.DC-DC Converter:

A DC-DC converter which interfaces between load and module is considered as the main part of a MPPT system, it serves the purpose of transferring maximum power from PV module to the load. By changing the Duty cycle (D), the load impedance as seen by the source (R_{in}) is varied and matched at the point of the peak power with the source so as to transfer the maximum power.

There are several topologies available for DC-DC converter, among them non-inverting buck-boost converter. The non-inverting buck-boost converter is a cascaded combination of a buck converter followed by a boost converter. Besides the aforementioned buck-boost mode, wherein S_1 and S_2 have identical gate-control signals, the non-inverting buck-boost converter also can operate in either buck or boost mode; by operating the converter in buck mode when V_s is higher than V_o , and in boost mode when V_s is lower than V_o , the buck-boost function is then realized [10].

Figure 2.3 shows the circuit topology of non-inverting Buck-Boost converter.

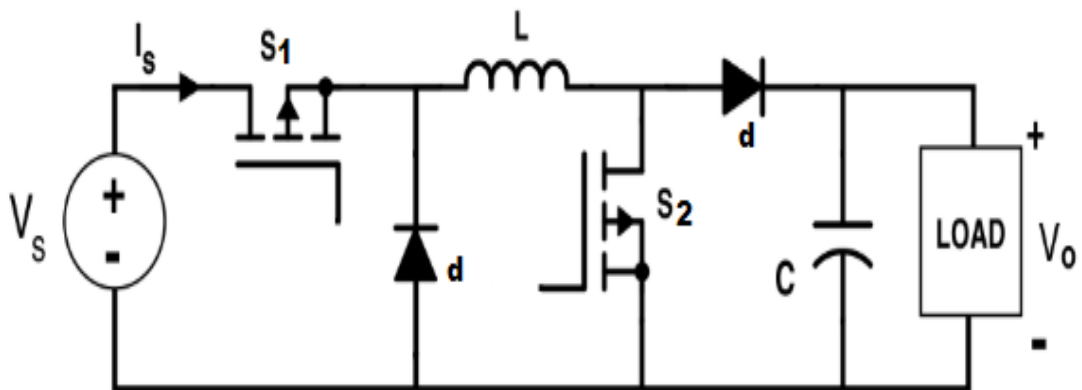


Figure 2.3: Non-inverting buck-boost converter. [10]

The diode (d) is used to enhance the output filtering effect and prevent the switches from absorbing or dissipating the inductive energy because this would lead to overheating the switches. In addition, the capacitor at the output of the converter is used to attenuate the output voltage fluctuation.

During the steady-state condition the relation between the input voltage V_s , the output voltage V_o and the duty ratio D of the converter can be defined by the following equation [10]:

$$\frac{V_o}{V_s} = \frac{D}{1-D} \quad (2.1)$$

Also, the relation between the input current I_{in} and output current I_o is defined by the following equation [10]:

$$I_{in} = \frac{D}{1-D} I_o \quad (2.2)$$

From equation (2.1) the output voltage could be higher or lower than the input voltage according to the value of the duty ratio. For the duty ratio condition $D > 0.5$, the output is higher than the input and the converter starts operating in boost mode. If $D < 0.5$ the output is lower than the input and the converter starts operating in buck mode.

The value of the inductor and the capacitor used in non-inverting buck-boost converter design are calculated by the following equations [10]:

$$C = \frac{D}{R_o f_s \left(\frac{\Delta V_o}{V_o}\right)} \quad (2.3)$$

$$L = \frac{(1-D)^2 R_o}{2 f_s} \quad (2.4)$$

The input impedance of the converter is given by equation (2.5) [11]:

$$R_{in} = R_o \frac{(1-D)^2}{D^2} \quad (2.5)$$

Where:

R_o : Output resistance or load resistance of the converter (Ω).

ΔV_o : Desired voltage ripple (V).

f_s : Switching frequency (Hz).

2.3.2.MPPT algorithms:

Numerous MPPT algorithms have been proposed to track the maximum power of PV panel. Even though these algorithms are proposed for the same purpose, they differ tremendously regarding efficiency, tracking speed, steady-state oscillations, complexity, hardware implementation, cost and track global MPP or not. Moreover, each method may work effectively in certain conditions while not in others. MPPT algorithms are classified into three groups:

-Indirect methods: namely Fractional Short-Circuit Current (FSCC), Fractional Open- Circuit Voltage (FOCV).

-Direct methods: such as Hill Climbing (HC), Perturb and Observe (P&O), and Incremental Conductance (INC), Kalman Filter, Fuzzy Logic Control (FLC), Neural Network (NN), and Partial Swarm Optimization (PSO) [21].

2.3.2.1. Perturb and Observe algorithm:

Perturb and Observe algorithm is a traditional and simple algorithm that widely used in early time of MPPT application. As its name suggests, it works by introducing a perturbation (offset) in the Duty cycle as shown in figure 2.4; it compares the current value of the power calculated by multiplying the voltage and current of PV module with the previous one. And then, according to the result of comparing the power, it compares the current sampling value of the voltage with the previous value in the same method and controls the Duty cycle to track the maximum power point.

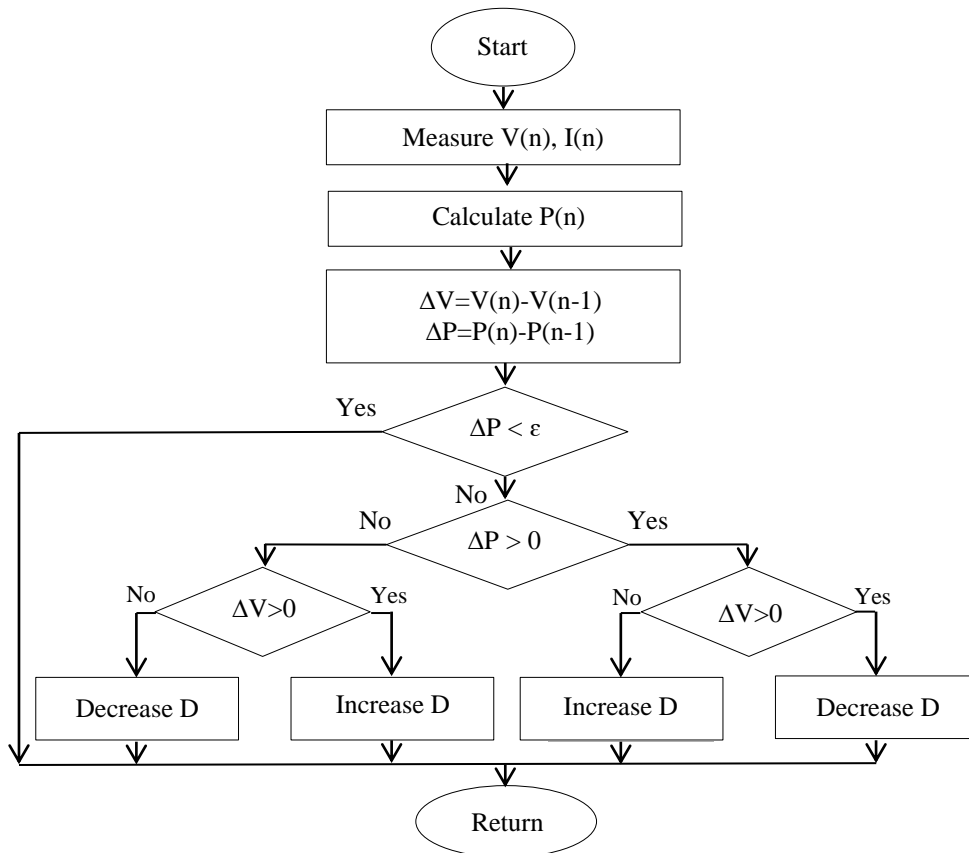


Figure 2.4: Flowchart of P&O algorithm.

Therefore, P&O algorithm uses the characteristic of the P-V curve as shown in figure 2.5. The initial operating point starts at the open-circuit voltage. When the operating point is located on the right side of the Maximum Power Point and then the P-V curve slope is negative, the Duty cycle is increased if ΔV is positive and it is decreased if ΔV is negative. On the other hand, if the P-V curve slope is positive and the operating point is located on the left side of the maximum power point, the Duty cycle is decreased if ΔV is positive and it is increased if ΔV is negative [22].

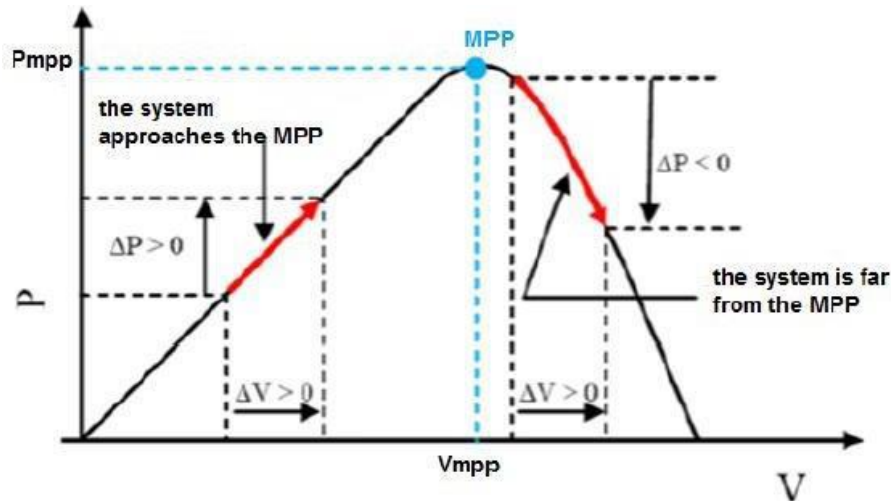


Figure 2.5: P&O schematic diagram. [23]

The amount of perturbation value ‘offset’ depends upon the nature of the algorithm. It can be constant or varying. Pertaining to this fact, two further groups of P&O method are available in the literature, namely fixed-step P&O and variable step P&O methods.

2.3.2.2. Particle Swarm Optimization:

Particle Swarm Optimization is a population based stochastic optimization technique developed by Dr.Eberhart and Dr.Kennedy in 1995, inspired by social behaviour of bird flocking or fish schooling. The system is initialized with a population of random solutions and searches for optima by updating generations. In PSO, the potential solutions called particles, fly through the problem space by following the current optimum particles.

The PSO algorithm defines initial position of a random particle swarm which are randomly distributed in the search space. After the algorithm starts, the particles update their velocity and position and find the optimal position iteratively. During iteration, each particle has a fitness value determined by an objective function, and a velocity

which the particle uses to determine the flight direction and distance. Particles calculate the direction and velocity of the next iteration based on the best position found by the particle itself (P_{besti}), which is stored as individual best solution, and the best position in the swarm (G_{best}), which is stored as the best global solution. These two extreme values are constantly updated as each particle's velocity and position are updated, and eventually stabilizing at the global extreme point [24].

In every iteration of the particle, the update formula of the velocity, position, P_{besti} and G_{best} of each particle is [25]:

$$V_i^{k+1} = wV_i^k + c_1r_1(P_{besti}^k - X_i^k) + c_2r_2(G_{best}^k - X_i^k) \quad (2.6)$$

$$X_i^{k+1} = X_i^k + V_i^{k+1} \quad (2.7)$$

$$P_{besti} = \begin{cases} P_{besti} & f(X_i) \geq f(P_i) \\ X_i & f(X_i) < f(P_i) \end{cases} \quad (2.8)$$

$$G_{best} = \max\{f(P_{best0}); f(P_{best1}); \dots \dots; f(P_{bestm})\} \quad (2.9)$$

$$i=1,2,3,\dots,m$$

Where:

m is the number of particles.

X_i and V_i are the position and velocity of particle i ,

k is the number of iterations.

w is the particle inertia weight.

c_1 and c_2 are learning factors.

r_1 and r_2 are random numbers between (0, 1).

In PV system, Particle Swarm Optimization is applied to the Maximum Power Point Tracking control of PV system where the objective function is set to the output power of PV array, also the sum of power of all modules. The position of the particle is set to the operating voltage of the system and the speed of the particle is set to the system's voltage increment. The current optimal value of the particle is set to the Maximum Power Point voltage of each particle in the system. The optimal solution of the population is set to the Maximum Power Point voltage of the system [26]. The concrete steps of PSO applying to MPPT method of PV system are summarized in the flowchart shown in figure 2.6 [25].

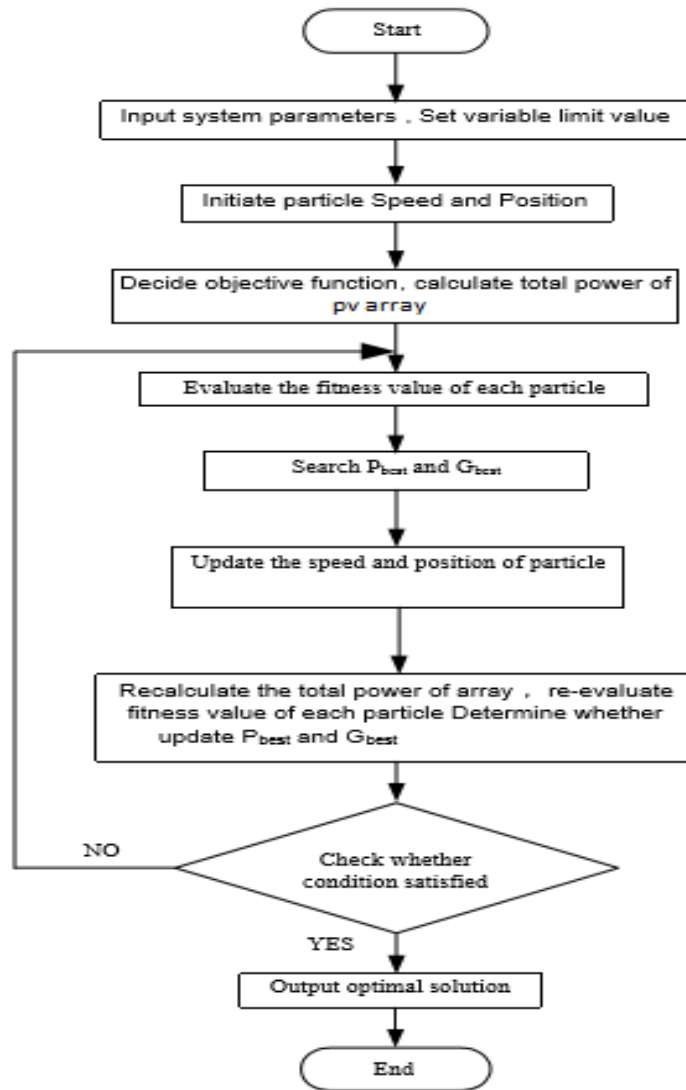


Figure 2.6: MPPT control based on PSO algorithm. [25]

2.4.Storage element:

The energy output from the Solar PV systems is generally stored in a battery or in a battery bank deepening upon the requirements of the system. Mostly batteries are used in the stand-alone system and in the case of grid connected system batteries are used as a backup system.

2.4.1.Battery types:

Battery is an energy storage device that consists of one or more electrochemical cells that transform stored chemical energy into electrical energy; this chemical energy is stored in its active materials through electrochemical reactions depending on the

desired nominal battery voltage and capacity Cells, which are connected in series, parallel or both. Batteries are generally classified into primary and secondary batteries.

Primary batteries are disposable batteries. They are built to be used only once and then discarded or recycled, this is because the chemical reactions that take place within primary batteries cannot be reversed, and the active materials do not go back to their original forms.

Secondary batteries, also called rechargeable batteries, are built to be recharged and reused many times. They usually include active materials that are assembled in a discharged state. These batteries can be recharged upon the application of electric current, which helps to reverse the chemical reactions that take place when the battery is used. Secondary batteries are of significant interest for their ability to store and supply energy [27].

2.4.2. Battery specifications:

- C-rate: the rate at which a battery can deliver or accept current, stated in terms of the rated capacity of the cell in amp-hours.

-The State Of Charge (SOC): is a measurement of the amount of energy available in a battery at a specific point in time expressed as a percentage (0% = empty, 100% = full).

-Depth Of Discharge (DOD): a measure of how much energy has been withdrawn from a battery, expressed as a percentage of full capacity. Depth Of discharge is the reciprocal of State Of Charge.

-Efficiency: is the ratio of the charge extracted during discharge cycle to the amount of charge stored during charge cycle.

-Self-discharge: the rate at which a battery discharges, or loses stored energy, due to internal cell reactions.

-State of Health (SoH): a metric that reflects the general condition of a battery and its ability to deliver the specified performance compared with a fresh battery. The unit of SoH is percent points (100% = the battery conditions match the battery specifications). It takes into account factors such as capacity, internal resistance, and self-discharge.

-Lifetime: is the number of cycle charge/discharge the battery can sustain before losing 20% of its nominal capacity [28].

2.4.3. Battery technologies:

Different technologies of batteries are manufactured today, each with specific design for particular applications. Each battery technology or design has its individual strengths and weaknesses. The selection of the suitable battery depends upon the application and the designer. In most cases Lead-acid and Lithium-ion are the best option for a solar panel system.

Lead-acid batteries are the most common batteries used in Photovoltaic system. This is due to their wide availability in many sizes, low cost and well determined performance characteristics. However, Lead-acid batteries have a relatively low cycle life and they require frequent maintenance.

Lithium-ion batteries (li-ion) are one of the most popular types of rechargeable batteries with one of the best energy-to-weight ratios, high open circuit voltage, low self-discharge rate and no memory effect. They can operate over a wide temperature range and have a long cycle life which makes them more suitable for PV system. One of the disadvantages of li-ion is that they have a moderately high initial cost [28, 29].

2.5. Charging controller:

A charging controller or charging regulator limits the rate at which electric current is added to from electric batteries. It prevents overcharging and may prevent against overvoltage, which can reduce battery performance or lifespan, and may pose a safety risk.

In simple words, the main function of the battery charging controller is to control the battery charging from solar cell and also control the battery drain by load. The Charging controller checks the battery whether it requires charging and starts charging the battery in one of many battery charging algorithms. Whenever controller found that the battery has reached the full charging voltage levels, it then stops the charging from solar cell.

The charging controller is composed of two main components DC-DC boost converter and battery charging algorithm. The DC-DC boost converter takes the role of traditional charger by controlling the current level and DC voltage. The Duty cycle of the converter switch is controlled by battery charging algorithms.

2.5.1.Boost converter:

Boost converter or step up converter has output voltage greater than input voltage and output current is smaller than the input current. The circuit topology of the step-up converter is illustrated in figure 2.7.

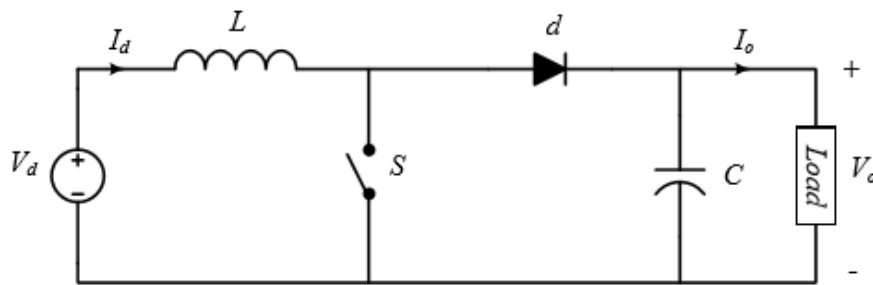


Figure 2.7: Boost converter circuit. [10]

When the switch S is on, the diode d is reverse biased. Consequently, the current in the inductor L rises linearly due to the input voltage source, and in this case the output stage is isolated and the capacitor C is partially discharged supplying the current load. When the switch is off during the second interval the diode is conducting, and during this time the output stage receives energy from both the inductor and the input source. When the converter is operating at steady-state condition, the duty ratio D can be expressed by equation 2.10. [10]

$$D = 1 - \frac{V_d}{V_o} \quad (2.10)$$

Where D denotes the duty ratio, V_d and V_o denotes the input and the output voltages of the converter, respectively. From the above equation it can be seen that, the increase in the duty ratio D will increase the value of the output voltage, V_o . In addition, the change in the duty ratio results in change in the input and the output current of the converter. The filter inductor and capacitor to operate the converter in the continuous conduction mode can be calculated by the following equations [10]:

$$L = \frac{V_d D}{2\Delta I f_s} \quad (2.11)$$

$$C = \frac{I_o}{\Delta V_o f_s} \quad (2.12)$$

Where:

ΔI : Desired current ripple (A).

ΔV_o : Desired voltage ripple (V).

f_s : Switching frequency (Hz).

2.5.2. Battery charging techniques:

Proper battery charging techniques can significantly improve battery performance and life cycles. Thus, several factors such as fast charging, good quality of charging current and avoiding under and over charging are considered. Therefore, an appropriate control technique for charging process should be adopted.

A number of techniques for charging batteries have been developed to meet the “rules for proper charging”. Some of these techniques are known as the Constant-Current technique (CC), Constant-Voltage technique (CV) and mixed Constant-Current and Constant-Voltage technique (CC-CV).

2.5.2.1. Constant-Current charging (CC):

Constant-Current technique is the most conventional battery charging techniques. As shown in figure 2.8 the battery current is kept constant while battery voltage increases during charging until it reached the allowed value V_{OCH} (rated voltage of the battery). When the battery voltage has reached its final value, the charging controller disconnects the battery from the converter to avoid overcharging and consequent battery failure. One of the main disadvantages of CC charging techniques is the overcharging risk which can occur when a high charging current is used.

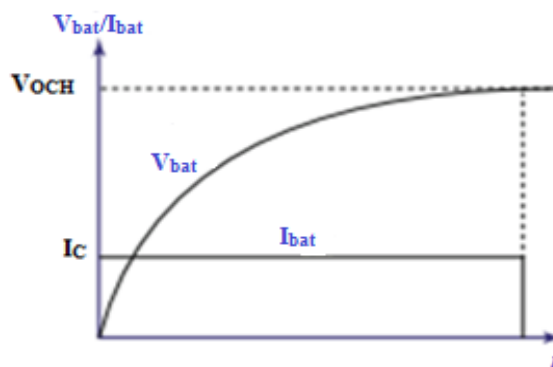


Figure 2.8: Constant-Current charging technique. [28]

2.5.2.2. Constant-Voltage charging (CV):

The charging characteristic curve of this technique is illustrated in figure 2.9. In this method, the battery voltage remains constant while the battery current is decreasing and eventually becomes very low. This initial current I_C temporarily increases the battery temperature and can degrade the battery. When the current reaches a specific amount I_{min} , the battery charging controller disconnects the battery from the charger circuit.

The main disadvantage of the CV charging methodology is the temperature rise which can damage the battery. Another drawback of CV charging is the long charge time due to the very low currents at the final stages of the charging.

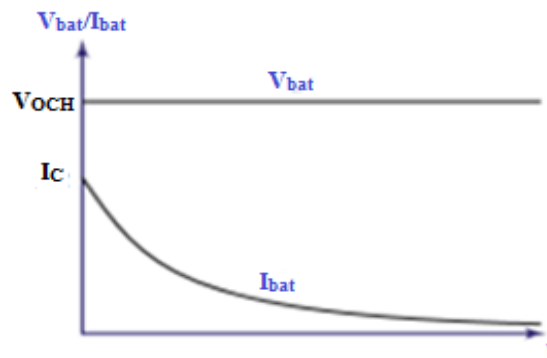


Figure 2.9: Constant-Voltage charging technique. [28]

2.5.2.3. Mixed Constant-Current and Constant-Voltage charging (CC-CV):

The CC-CV charging technique utilizes both CC and CV charging. As shown in figure 2.10 the charging is performed in 2 stages. In the first stage, the charger provides constant charging current I_C until the battery's voltage reaches a predetermined value V_{OCH} . Then in the second stage, the current decreases until it reaches a specific amount I_{min} . The battery charging controller disconnects the battery from the charger circuit when the battery current reaches I_{min} .

Since the current is kept constant at the first charging stage, the current rush disadvantage of CV charging technique is avoided. Also, since the voltage is kept constant at the second stage, the overcharging disadvantage of CC charging is avoided. These advantages of CC-CV charging technique make it perfect for applications for high performance requirement [28, 30].

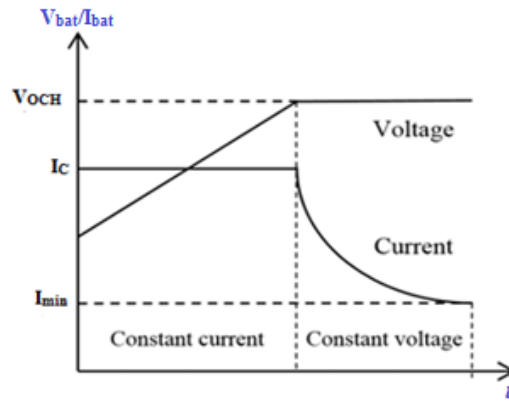


Figure 2.10: CC-CV charging technique. [28]

The corresponding algorithm of CC-CV charging technique is shown in figure 2.11.

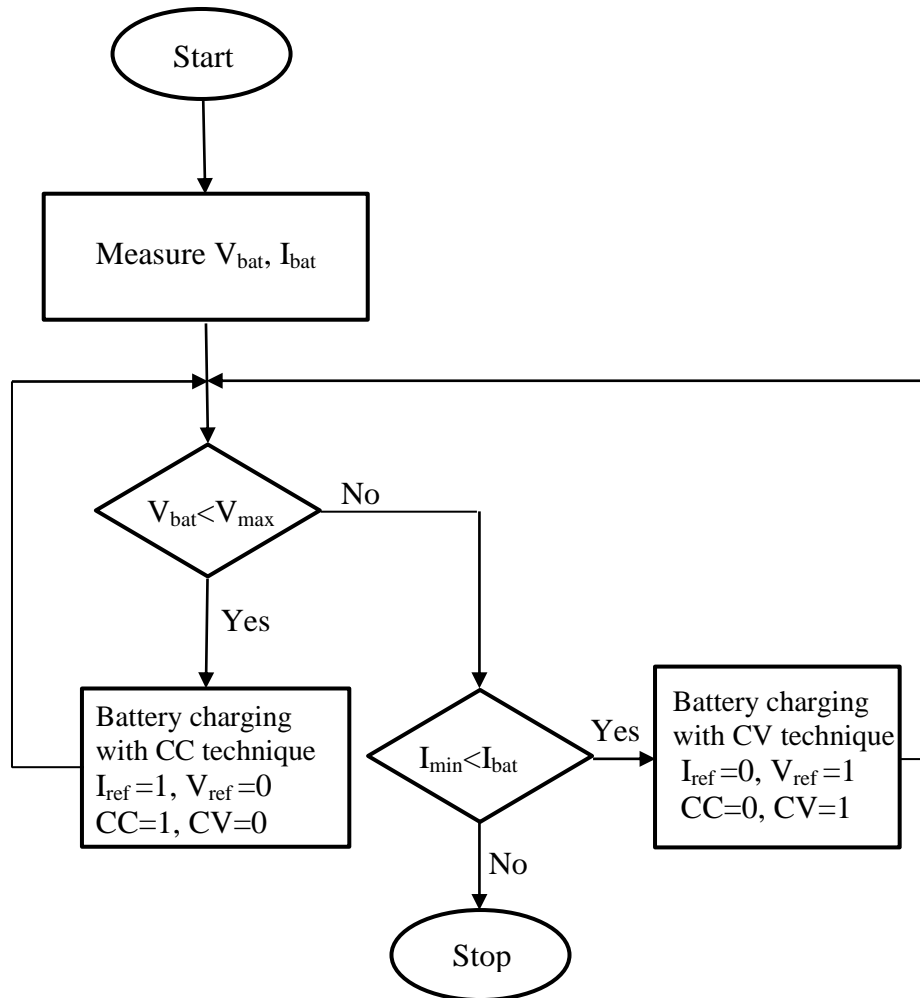


Figure 2.11: CC-CV battery charging technique flowchart.

2.6.Conclusion:

This chapter has shown the different MPPT algorithms used to locate the Maximum Power Point of the PV modules. Also, the main function of the charge controller has been discussed and different techniques of proper battery charging has been presented.

Chapter three:

Simulation and results

3.1.Introduction:

This chapter describes how the SIMULINK models of the proposed PV systems were implemented to test and verify the functionality of the proposed MPPT algorithms and battery charging controller. Two different PV systems were implemented in MATLAB/SIMULINK environment. The first system was implemented with a resistive load to evaluate the effectiveness and the advantages of the proposed P&O and PSO algorithms. The second PV system was also simulated in MATLAB, but the resistive load was replaced with a battery to demonstrate the feasibility and performance of the proposed battery charging controller.

3.2.PV array characteristics:

To simulate the PV system described in chapter two a Xunlight XR36-300 PV module was used. Specifications of the chosen module are shown in figure 3.1.

| Module data | | Model parameters |
|---|---|------------------------------------|
| Module: Xunlight XR36-300 | | Light-generated current I_L (A) |
| Maximum Power (W) | Cells per module (Ncell) | 6.7045 |
| 300 | 36 | Diode saturation current I_0 (A) |
| Open circuit voltage V_{oc} (V) | Short-circuit current I_{sc} (A) | $1.9382e-10$ |
| 81 | 6.35 | Diode ideality factor |
| Voltage at maximum power point V_{mp} (V) | Current at maximum power point I_{mp} (A) | 3.6458 |
| 60 | 5 | Shunt resistance R_{sh} (ohms) |
| Temperature coefficient of V_{oc} (%/deg.C) | Temperature coefficient of I_{sc} (%/deg.C) | 49.5556 |
| -0.38 | 0.12101 | Series resistance R_s (ohms) |
| | | 2.2134 |

Figure 3.1: PV module specifications.

3.2.1.Under normal conditions:

Figure 3.2 and 3.3 represent SIMULINK model of single PV module and its corresponding I-V and P-V characteristics curves under normal conditions.

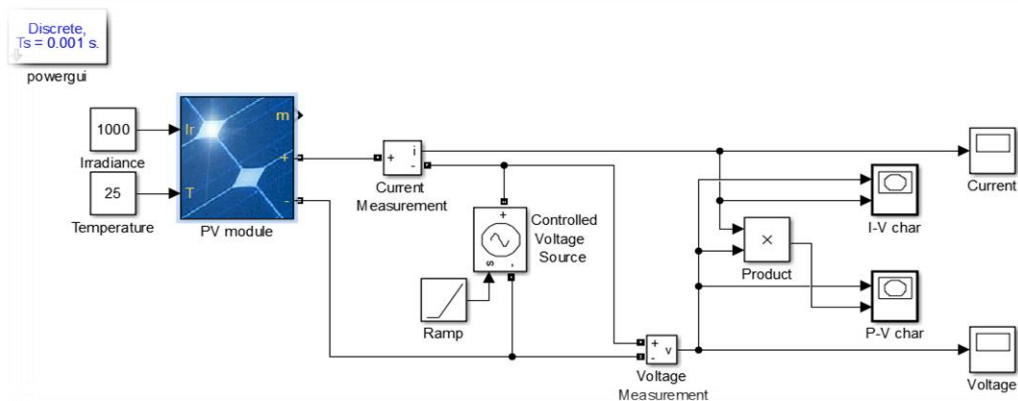


Figure 3.2: SIMULINK model of single PV module.

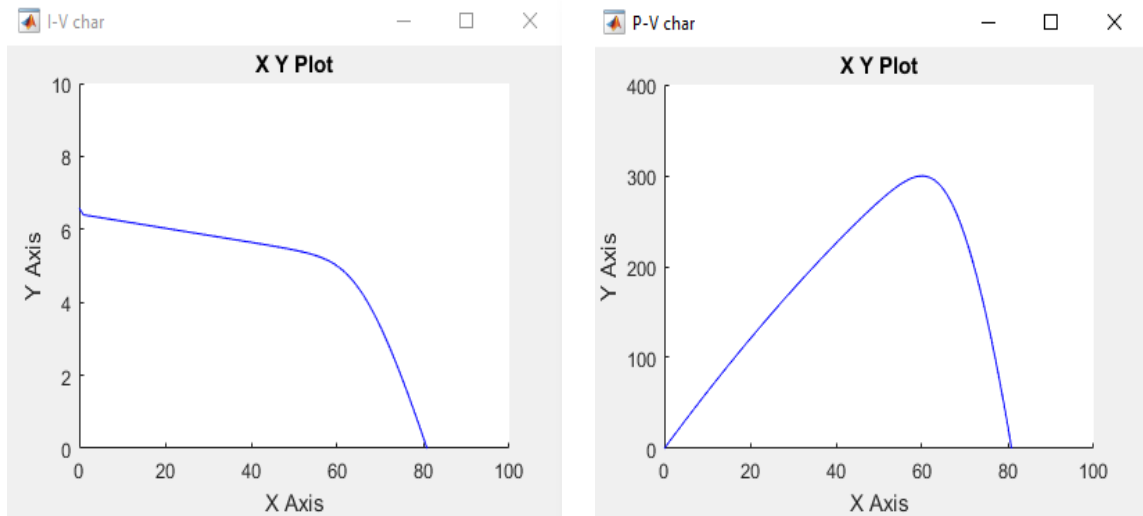


Figure 3.3: I-V and P-V characteristics of single PV module.

Figure 3.4 and 3.5 show the model of three PV modules connected in series and its corresponding I-V and P-V characteristics curves.

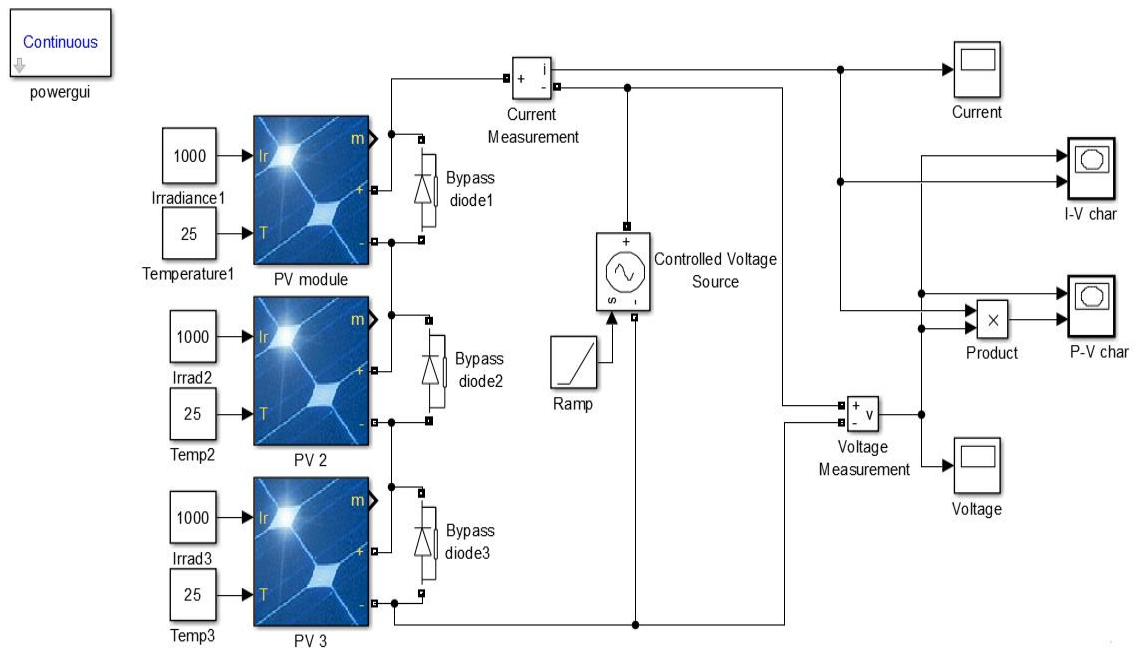


Figure 3.4: SIMULINK model of three PV modules in series under uniform conditions.

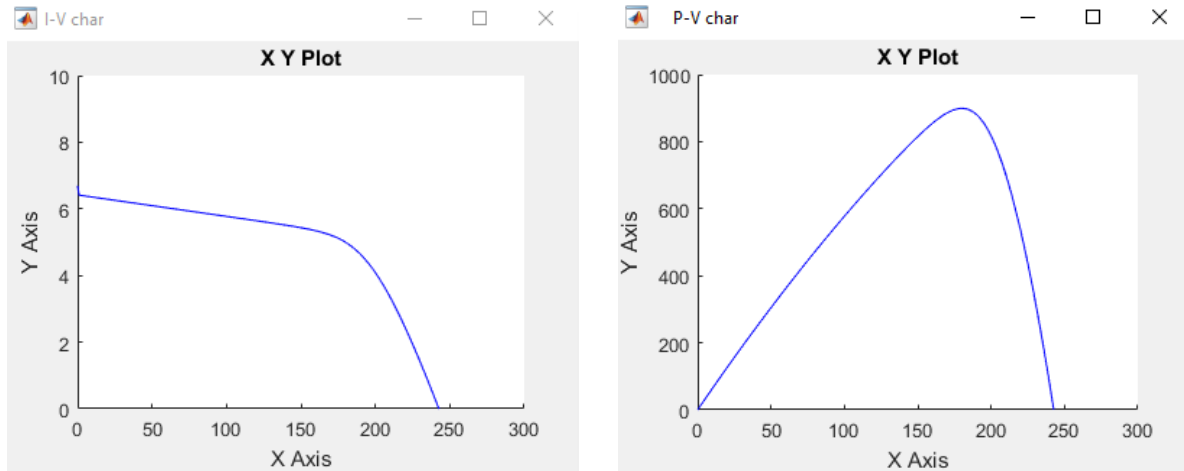


Figure 3.5: I-V and P-V characteristics of three PV modules in series.

As can be seen from the simulation results shown in figures 3.3 and 3.5, the voltage and the maximum power of three modules under uniform irradiance are triple of the ones of single PV module.

3.2.2. Under climate changing conditions:

3.2.2.1. Irradiance effect:

Figure 3.6 shows the effect of irradiance on I-V and P-V characteristics curves, where the current increases with the increase of solar irradiance and vice versa.

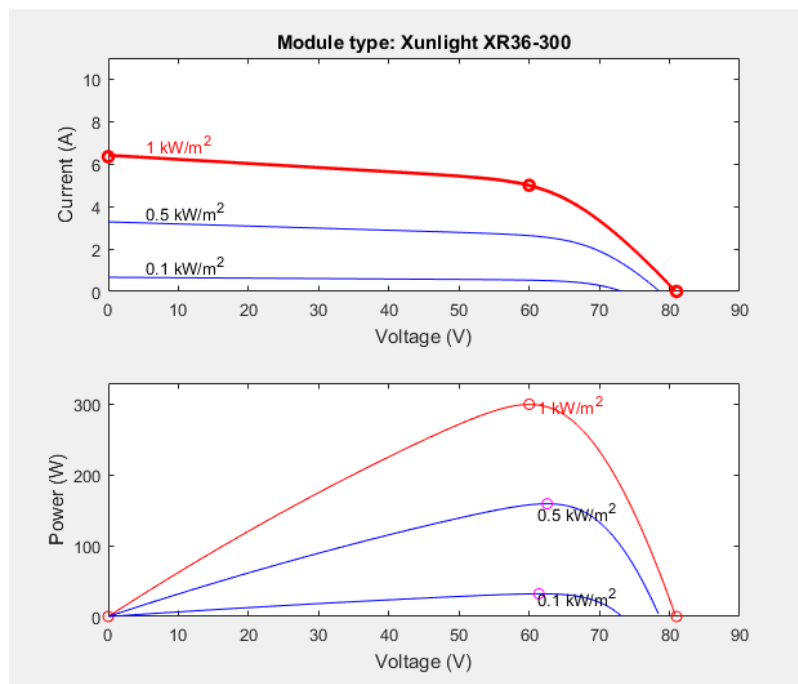


Figure 3.6: Irradiance effect on I-V and P-V characteristics curves.

3.2.2.2. Temperature effect:

As can be observed in figure 3.7 the voltage increases when the temperature decreases.

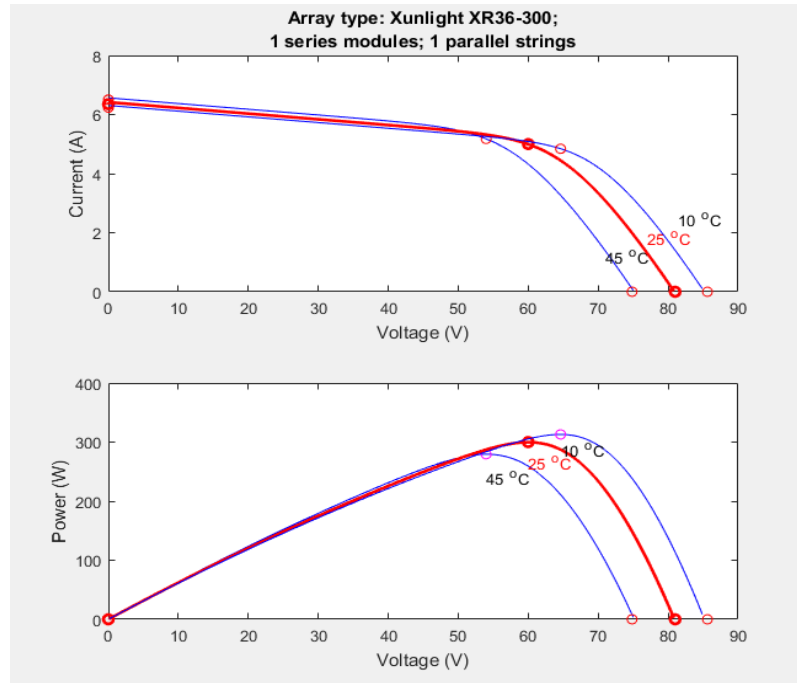


Figure 3.7: Temperature effect on I-V and P-V characteristics curves.

3.2.3. Under partial shading condition:

To show the effect of the non-uniform solar irradiance on the PV characteristic of the PV modules, the model shown in figure 3.8 was simulated.

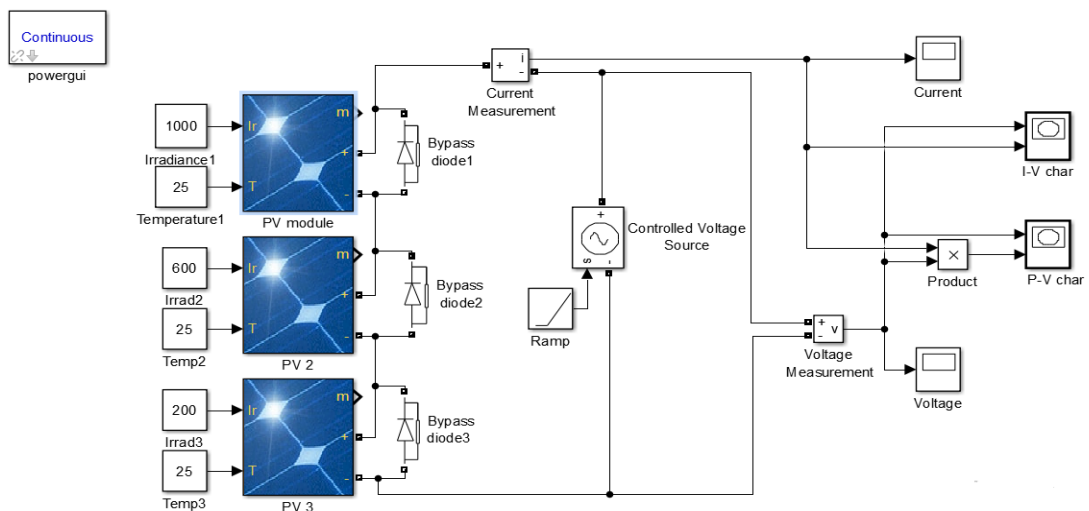


Figure 3.8: SIMULINK model of three PV modules in series under non-uniform conditions.

The P-V characteristic curve shown in figure 3.9 develops multiple maxima when the PV modules are partially shaded due to bypass diodes effect.

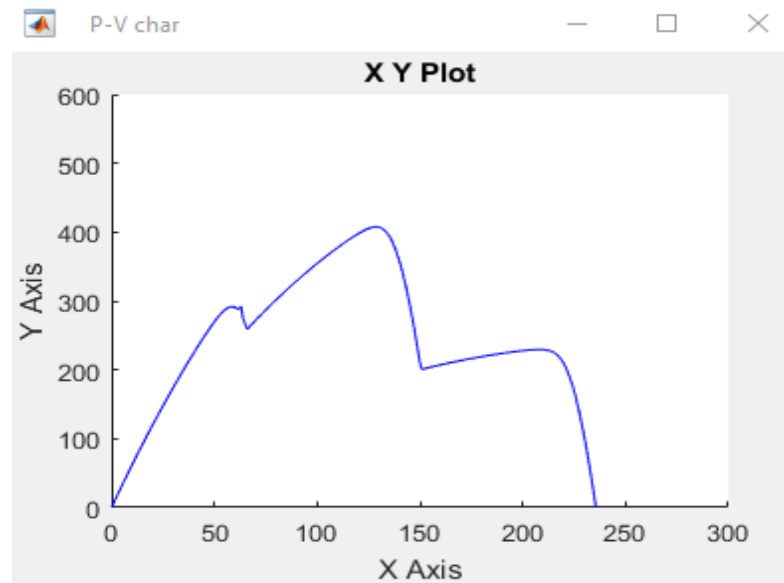


Figure 3.9: P-V characteristic curve of PV modules under partial shading.

3.3. Maximum Power Point Tracker:

In order to extract the maximum power from the PV array that contains three PV modules connected in series the SIMULINK model shown in figure 3.10 was simulated

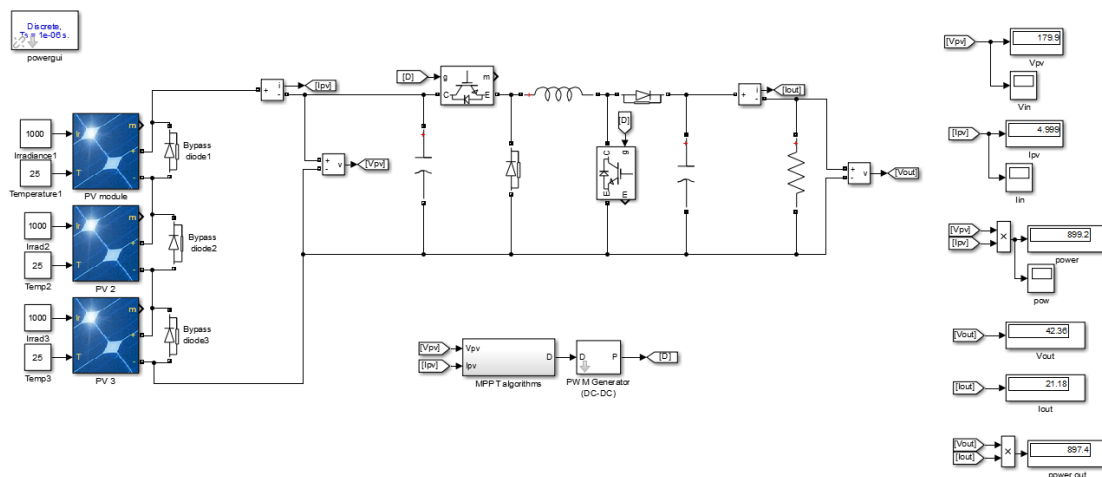


Figure 3.10: SIMULINK model of PV system with MPPT algorithm.

In this simulation P&O and PSO algorithms were tested, these algorithms are responsible to generate the appropriate Duty cycle which is used to control buck-boost converter switches.

The parameters of the components used to model the non-inverting DC-DC buck-boost converter were calculated using the equations mentioned before and they are listed in table 3.1

Table 3.1: Buck-boost parameters.

| Frequency | Resistor | Inductor | Input capacitor | Output capacitor |
|-----------|------------|----------|-----------------|------------------|
| 5000 Hz | 2 Ω | 2 mH | 1600 μ F | 100 μ F |

The simulations offer an opportunity to verify the performance of the proposed algorithms. For evaluation and comparison analysis, the simulation studies were carried out under steady-state and dynamic conditions for the proposed PSO and conventional P&O algorithms, by configuring the simulations under exactly the same conditions.

In reality, the output power of a Photovoltaic cell is mainly influenced by ambient temperature and solar irradiation, although the change in ambient temperature has a slow influence on the PV cell and it is not directly related to the speed of dynamic response. Therefore, the cell working temperature was fixed at 25 °C in all simulations. However, in practice the irradiance is not always constant because of climate changing and partial shading phenomenon which lead to a sudden change in the PV panel output power. Consequently, the algorithm had to be tested under different irradiation levels to verify the speed of tracking.

The PV array was expected to produce 900W with MPPT voltage and current of 180V and 5 A respectively at 1000 W/m² solar irradiance.

In order to study the performance of the algorithms under climate changing conditions the irradiance signal was set as shown in figure 3.11.

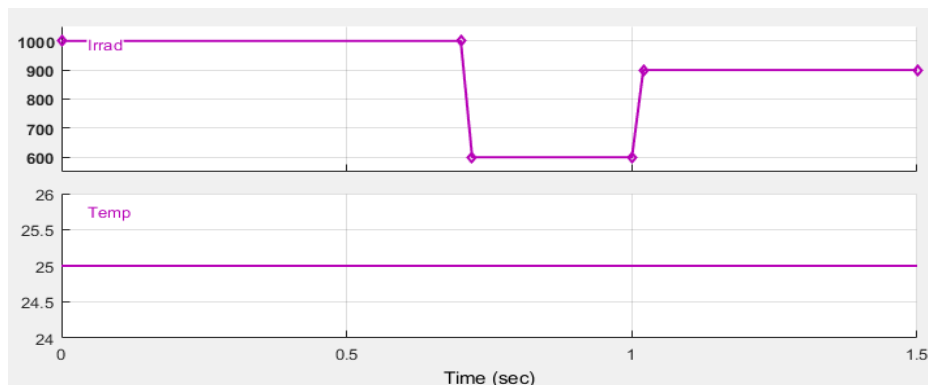


Figure 3.11: Irradiance and temperature signals.

To test P&O and PSO algorithms under partial shading phenomenon the three PV modules were set to constant temperature (25 °c) and different irradiance (irr 1=1000 W/m², irr 2=600 W/m² and irr 3=200 W/m²). The PV array was expected to produce power of 400 W, voltage of 80 V and current of 5 A at the global maximum power point.

3.3.1.Perturb and Observe algorithm simulation:

The conventional Perturb and Observe algorithm which was introduced in chapter two was written as M-file code based on its algorithm in embedded MATLAB function. The initial values of the P&O parameters were defined in table 3.2.

Table 3.2: Initializing P&O parameters.

| Dinit | Dmax | Dmin | Ddelta |
|-------|------|------|--------|
| 0.6 | 0.8 | 0.1 | 0.01 |

The simulation results of the PV system presented in figure 3.10 with MPPT P&O algorithm under uniform conditions are shown in figures from 3.12 to 3.14.

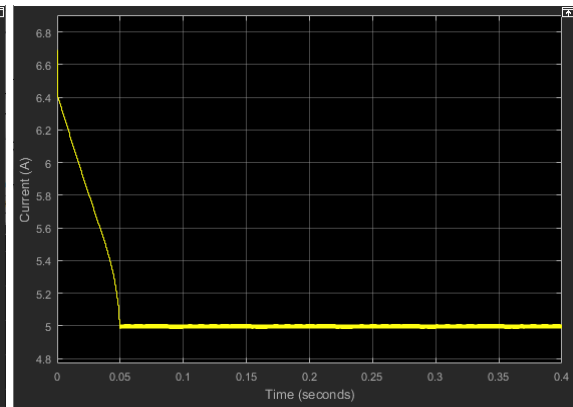
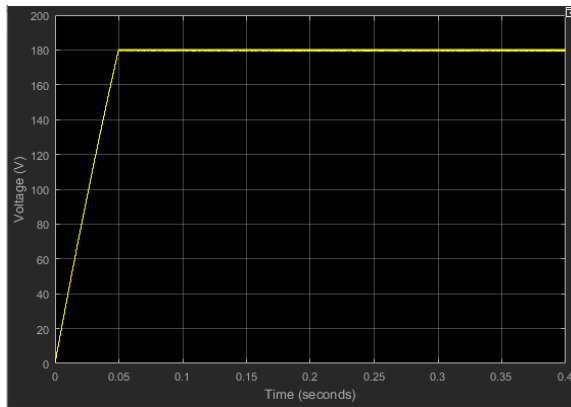


Figure 3.12: Voltage waveform using P&O under fixed irradiance.

Figure 3.13: Current waveform using P&O under fixed irradiance.

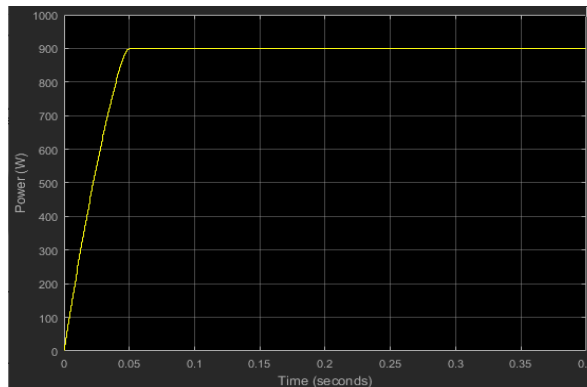


Figure 3.14: Power waveform using P&O under fixed irradiance.

The simulation results show a good performance in tracking the maximum power point. The P&O algorithm convergence time to the steady state is small; it takes only 0.05s to reach the MPP. However, the simulation results demonstrate small oscillation in voltage, current and power waveforms during the steady-state. This is because the P&O MPPT uses a fixed step-size to adjust the duty ratio.

The simulation of the model under varying irradiation levels (figure 3.11) gives the results waveforms shown in figures from 3.15 to 3.17.

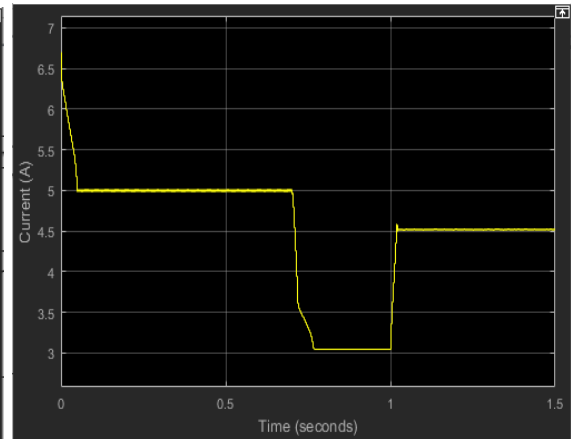
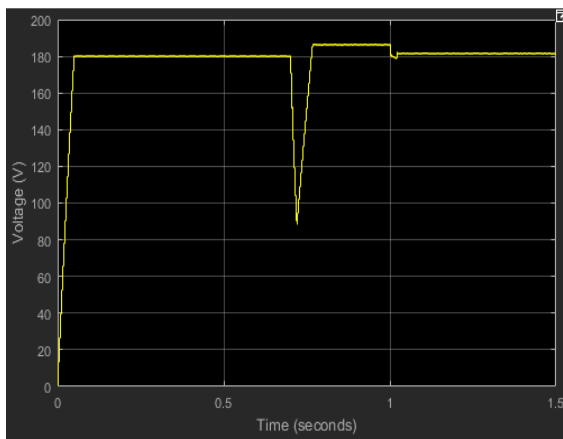


Figure 3.15: Voltage waveform using P&O under varying irradiance. **Figure 3.16:** Current waveform using P&O under varying irradiance.

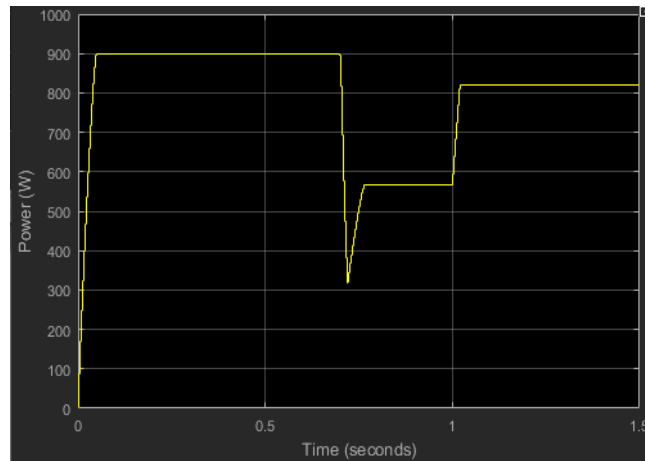


Figure 3.17: Power waveform using P&O under varying irradiance.

As seen from the results the simulated P&O algorithm can track the MPPT in each change of irradiance.

In the first change it can be seen that the P&O algorithm lost tracking and then restart immediately to find the new MPP because the accumulated move of the operating point is large.

Figures from 3.18 to 3.20 show the simulation results of the SIMULINK model when the PV array is partially shaded.

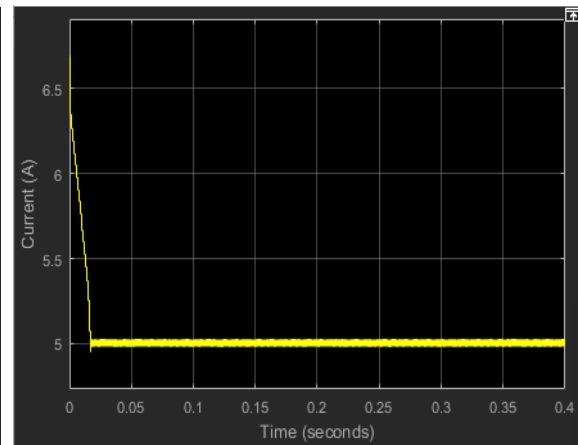
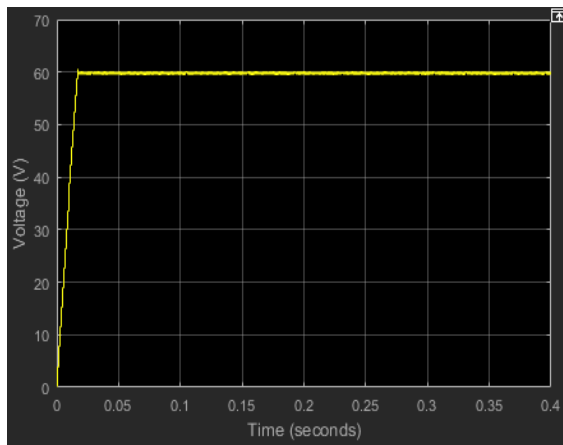


Figure 3.18: Voltage waveform using P&O **Figure 3.19:** Current waveform using P&O under shaded condition.

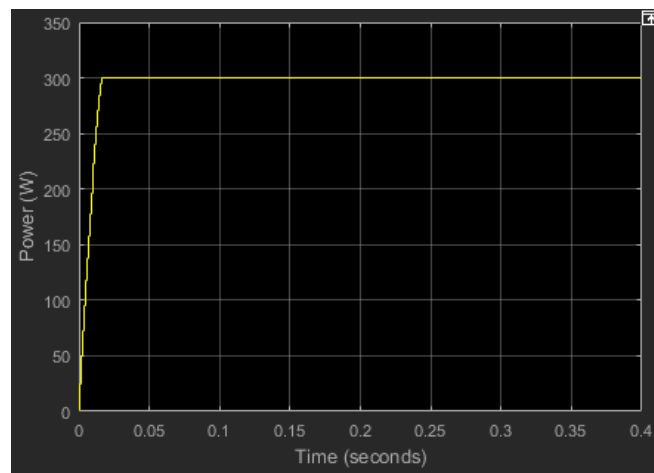


Figure 3.20: Power waveform using P&O under shaded condition.

From figure (3.18, 3.19 and 3.20) it can be seen that the P&O algorithm failed to track the global MPP; though it converged to the first peak of figure 3.9.

3.3.2. Particle Swarm Optimization simulation:

In this part P&O was replaced by PSO algorithm. It was simulated under uniform conditions and partially shading condition.

Table 3.3: Initializing PSO parameters.

| Number of Iterations | Swarm size | Initial duty cycle | Initial velocity | P_{best} of D | G_{best} of D |
|----------------------|------------|--------------------|---------------------|-----------------|-----------------|
| 15 | 3 | [0.25 0.4 0.7] | [0.001 0.001 0.001] | [0 0 0] | 0 |

The simulation results are shown in figures 3.21, 3.22 and 3.23.

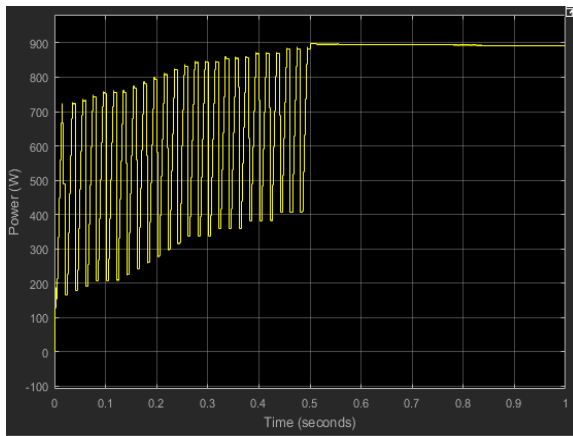


Figure 3.21: Power waveform using PSO under fixed irradiance.

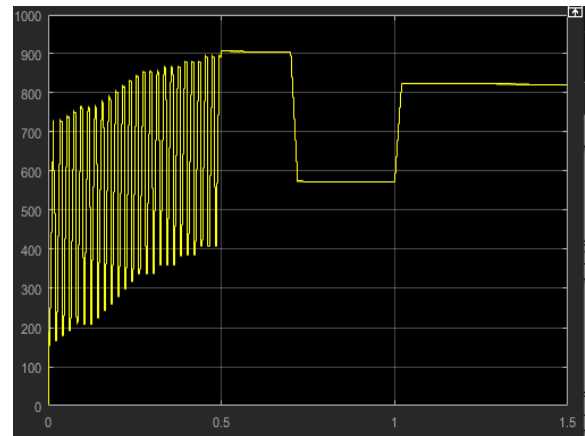


Figure 3.22: Power waveform using PSO under varying irradiance.

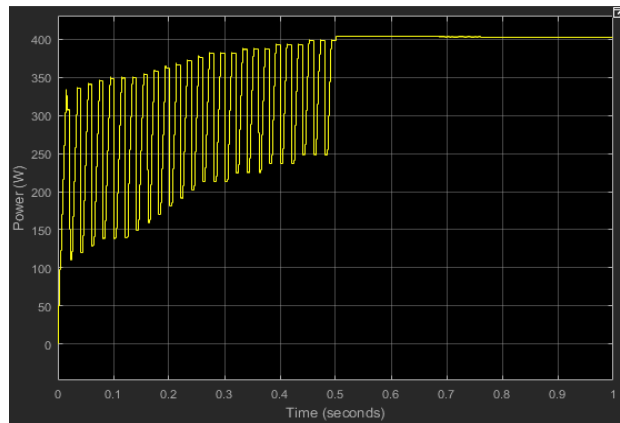


Figure 3.23: Power waveform using PSO under shaded condition.

From the results PSO algorithm can successfully track the Maximum Power Point under uniform conditions however the tracking speed is a little bit slow.

The PSO method can effectively avoid the local maximums and track the global Maximum Power Point under partial shading condition.

3.3.3.Comparison:

Table 3.4: Comparison of MPPT algorithms.

| | Uniform conditions | | Partial shading condition | |
|---------------------|--------------------|--------|---------------------------|--------|
| | P&O | PSO | P&O | PSO |
| P_{MPP} | 900 W | | 407.6 W | |
| Extracted P_{MPP} | 899 W | 897.2W | 299.7W | 404.5W |
| Efficiency | 99.89% | 99.69% | 73.53% | 99.24% |
| Tracking speed | 0.05 s | 0.5 s | 0.017 s | 0.5 s |

From table 3.3 it can be noticed that P&O algorithm converges faster to the steady state than PSO. However, under partial shading condition the P&O failed to track the global Maximum Power Point while the PSO algorithm did successfully.

Also the previous results confirm that PSO algorithm can effectively track the MPP under varying irradiance whatever the amount of irradiation change was compared to P&O.

4.1.PV system with battery charging controller:

The complete simulation model of the system consists of some masked blocks connected together as shown in Figure 3.24. The simulation was conducted by connecting a PV model, through a charging controller, to battery. Also, a MPPT control unit was included. The system was simulated to verify the functionality and performance of the proposed CC-CV charging method with P&O MPPT controller.

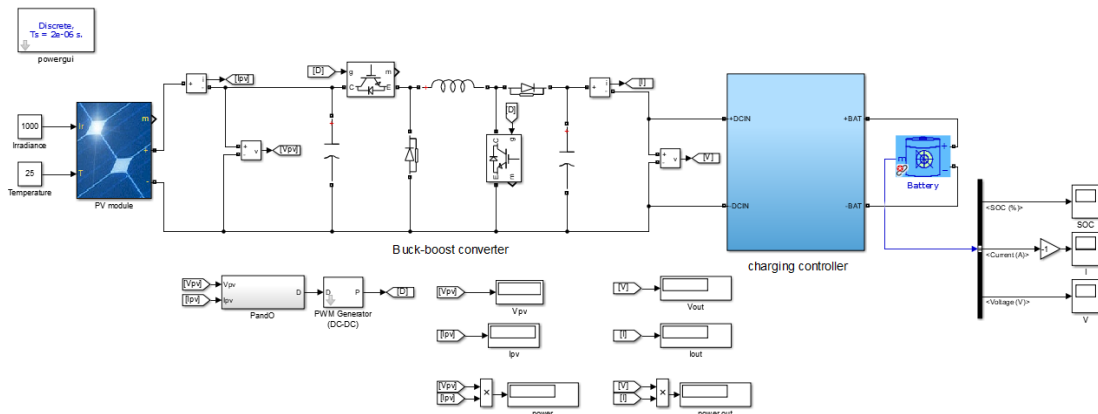


Figure 3.24: SIMULINK model of PV battery charging system with MPPT.

The SIMULINK models of the PV array and the MPPT controller are the same as simulated in the previous section. The battery used is a lithium-ion 24V 100Ah.

The characteristics of the simulated battery are shown in table 3.4.

Table 3.5: Battery characteristics.

| Nominal Voltage | Charge Voltage V_{OCH} | Charge current I_C | I_{MIN} | Rated capacity | Internal resistance | Cut-off voltage |
|-----------------|--------------------------|----------------------|-----------|----------------|---------------------|-----------------|
| 25.6 V | 29.2 V | 50 A | 5 A | 100 Ah | 0.0048 Ω | 36 V |

The SIMULINK block of the charging controller is illustrated in figure 3.25.

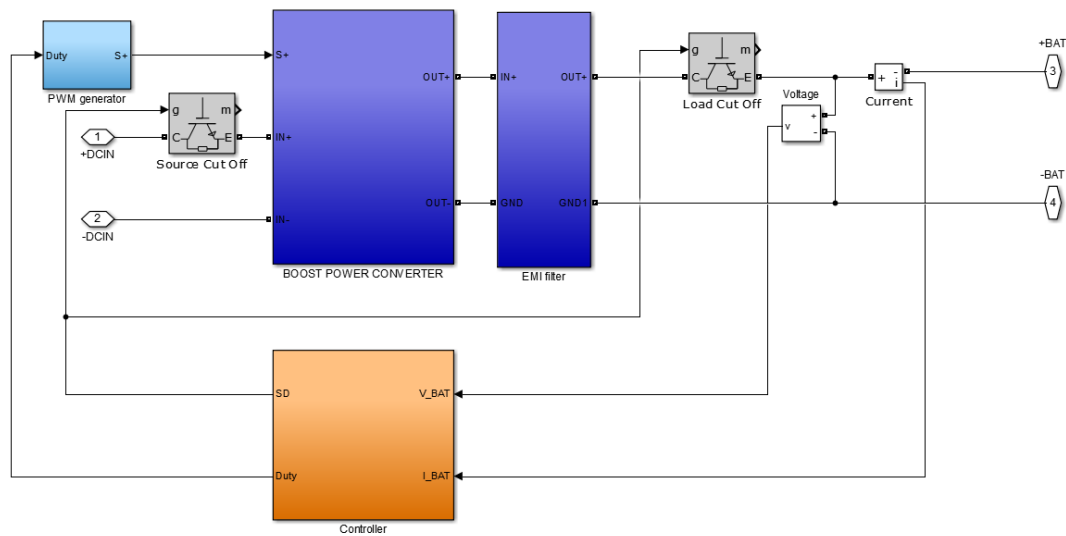


Figure 3.25: The SIMULINK model of the charging controller.

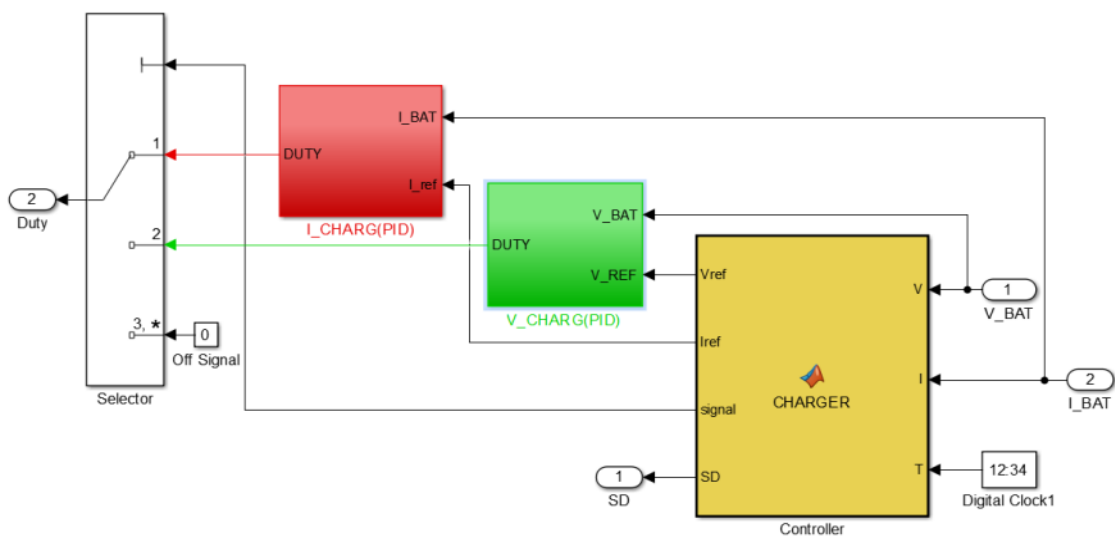


Figure 3.26: SIMULINK model of CC-CV controller.

Figure 3.26 shows the SIMULINK model of CC-CV controller.

Figures from 3.27 to 3.29 show the battery SOC, current and voltage during the charging process.

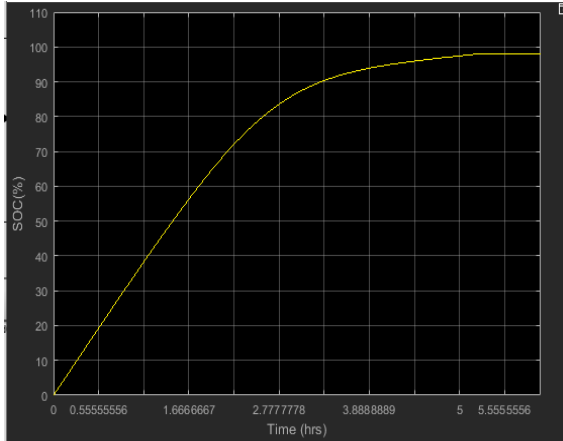


Figure 3.27: State Of Charge.

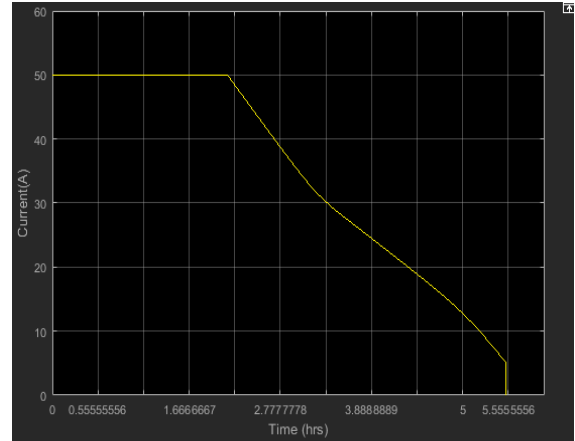


Figure 3.28: Battery charging current.

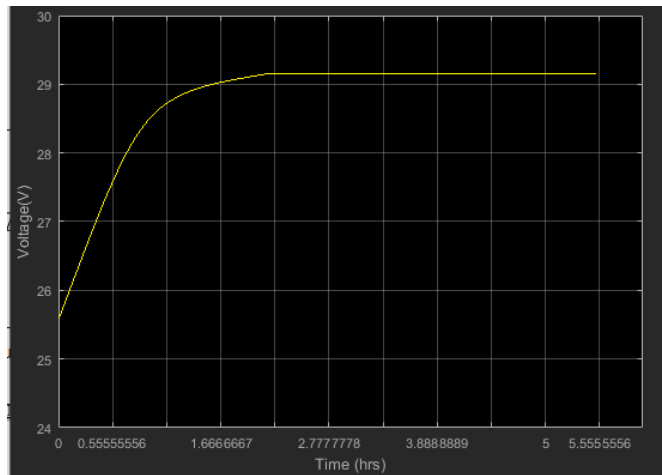


Figure 3.29: Battery charging voltage.

As can be seen from the results the battery first starts charging by CC charging technique. Where it charges with charging current I_c (50A). In this step of charging, the panel is working at MPPT and is supplying charging current to battery until battery voltage reaches maximum value of overcharging voltage, defined by V_{OCH} (29.2V). In this stage of charging battery has charge 70% SOC but there is still charging require to reach SOC 100%. So, the CC-CV algorithm switched to CV charging technique through the selector.

In CV charging stage, the output voltage of boost converter is regulated around V_{OCH} . That is achieved by sensing output voltage of the converter and comparing it with V_{OCH} . In this region battery keeps charging until current of battery falls below I_{min} (5A) and voltage stays in the value of V_{OCH} . In this region battery charges up to 98% of SOC. To protect the battery from over charging the algorithm activates SD signal to disconnect the battery from the PV array.

The battery takes only 5.5 hours to fully charge (CC stage: 2.10h, CV stage: 3.40h) due to CC-CV charge technique and Maximum Power Point Tracking.

4.2. Conclusion:

The simulations offered a valuable opportunity to verify the feasibility and the performance of the proposed PV system. For evaluation and comparison analysis, the simulation studies were carried out under exactly the same conditions for the proposed PSO and conventional P&O. the result proved that the P&O is better than PSO under normal conditions. However, under partial shading condition PSO is more efficient since it converged to the global Maximum Power Point while P&O did not.

Also, the battery charging controller CC-CV technique based has been tested and the results showed a satisfactorily performance.

General conclusion

General conclusion

In this research, a Photovoltaic system is presented to charge a battery. The main focuses of this research were how to improve the total system efficiency by implementing an efficient MPPT technique to extract the maximum available power from PV panels under changing atmospheric conditions. Also enhance the charging time of the battery and assure safe and complete battery charging process in order to increase the life span of the battery.

The two proposed MPPT algorithms P&O and PSO are simulated and tested using MATLAB/SIMULINK. The performances of the two algorithms were compared under changing irradiation levels and partial shading condition. The comparative study considers three important features: the Maximum Power Point Tracking speed, steady-state oscillation and global maximum power point. The simulation results showed that the P&O was more efficient compared with PSO algorithm under uniform irradiation. However, under non uniform irradiation it failed to track the global MPP while the PSO did successfully.

The charging controller is added to the system in order to charge the battery faster and protect it from over charging. The CC-CV charging technique was simulated and the result was presented in order to show the performance and the functionality of this method.

The implementation part of the proposed PV system was supposed to be done but due to CORONA virus pandemic it was cancelled.

Farther work of this project can be made by improving the algorithms to enhance the stability and the fast tracking capability under different conditions. Another improvement can be done by charging the battery with all four charging steps that are: soft charging, Constant-Current charging, Constant-Voltage charging and float charging. The system also can be developed to a complete standalone PV system.

References

- [1]. *Electronics*. (n.d.). Retrieved from DAEnotes:
<http://www.daenotes.com/electronics/industrial-electronics/solar-cell-working-construction>
- [2]. solar cell. (2020, april 1). Retrieved from Electrical 4 U:
<https://www.electrical4u.com/solar-cell/>
- [3] *learning center*. (s.d.). Récupéré sur samlexsolar:
<https://www.samlexsolar.com/learning-center/solar-cell-module-array.aspx>
- [4]. Krismadinata, Nasrudin, A. R., Hew, W. P., & Jeyraj, S. (2012). Photovoltaic module modeling using simulink/matlab. *Sustainable Future for Human Security*, (pp. 537-546). Kuala Lumpur, Malaysia.
- [5]. A. Durgadevi, S. Arulsevi, & S.P.Natarajan. (2011). Photovoltaic Modeling and Its Characteristics. *Emerging Trends in Electrical and Computer Technology*, (pp. 469-475). Nagercoil, India.
- [6]. (2018). *PV Module Parameters Identification Using Global Search Algorithms*. IGEE, Algeria.
- [7]. Photovoltaic array. (s.d.). Récupéré sur ALTERNATIVE ENERGY TUTORIALS:
<https://www.alternative-energy-tutorials.com/solar-power/pv-array.html>
- [8]. Photovoltaic or solar cell. (s.d.). Récupéré sur Circuit globe:
<https://circuitglobe.com/photovoltaic-or-solar-cell.html>
- [9]. N.ZERROUKI, & G.DAHMAN. (2019). *Control of Stand-Alone PV System Under Non-Uniform Irradiance*. IGEE, Algeria.
- [10]. Aashoor, F. (2015). Maximum Power Point Tracking techniques for photovoltaic water pumping system. University of Bath.
- [11]. V.C.Kotak, & Preti, T. (2013). DC to DC Converter in Maximum Power Point Tracker. *IJAREEIE*, 6115-6125.
- [12]. Djalab, A., Bessous, N., Rezaoui, M., & Merzouk, I. (2018). Study of the Effects of Partial Shading on PV Array. *Communication and Electrical Engineering*. EL Oued, Algeria.
- [13]. Seyedmahmoudian, M., Mekhilef, S., Rahmani, R., Yusof, R., & Renani, E. (2013). Analytical Modeling of Partially Shaded Photovoltaic Systems. *energies*, 128-144.
- [14]. Bypass Diodes in Solar Panels. (s.d.). Récupéré sur Electronics Tutorials:
<https://www.electronics-tutorials.ws/diode/bypass-diodes.html>

- [15]. J.Gosumbonggot, & G.Fujita. (2019). Partial Shading Detection and Global MPPT Algorithm for Photovoltaic with the Variation of Irradiation and Temperature. *energies*, 2-22.
- [16]. Newkirk, M. (2016, December 2). How solar works. Récupéré sur CLEAN ENERGY REVIEWS:
<https://www.cleanenergyreviews.info/blog/2014/5/4/how-solar-works>
- [17]. Joydib, J., Hiranmay, S., Konika Das, B., & Hiranmay, S. (2016). A Four Stage Battery Charge Controller on a Novel Maximum Pwer Point Tracking Based Algorithm for Solar PV System. 21st Century Energy Needs-Materials,Systems and Applicatioans. Kharagpur,India.
- [18]. H.A.Mohamed, H.A.Khatib, A.Mobarka, & G.A.Morsy. (2016). Design, Control and Performance Annalysis of DC-DC Boost Converter for Stand-Alone PV System. Eighteenth International Middle East Power System Conference. Cairo,Egypt.
- [19]. Hiwale, A., Patil, M., & Vinchurkar, H. (2014). An Efficient MPPT Solar Charge Controller. *IJAREEIE*, 10505-10511.
- [20]. M.Azah, & S.Hussain. (2011). Hopfield Neural Network Optimized Fuzzy Logic Controller for MPPT in a Photovoltaic System. *International Jornal of Photoenergy*.
- [21]. Saad, M., Aboubakr, E. H., & Ghzizal, A. E. (2019). The Most Used MPPT Algorithms: Review and the Suitable Low-cost Embedded Board for Each Algorithm. *Cleaner Production*.
- [22]. Lee, J., Jo, J., & Cha, H. (2018). MPPT Performance Comparison between Duty-Cycle Control and Current Control for Photovoltaic Power Conditioning System. *Electrical Machines and Systems*, (pp. 1036-1040). Jeju, Korea.
- [23]. A.Soufi, & A.Mohammadi. (2018). *Evaluation of Global MPPT for stand-alone PV System*. IGEE,Algeria.
- [24]. Guihua, L., Jianing, Z., Hailiang, T., Wei, W., & FRede, B. (2019). MPPTAlgorithm Based on PSO for PV Array Under Partially shaded Condition. *Electrical Machines and Systems*. Harbin,China.
- [25]. Ze, C., Hang, Z., & Hongzhi, Y. (2010). Research on MPPT Control of PV System Based on PSO Algorithm. *Chinese Control and Decision Conference* , (pp. 887-892). Xuzhou,China.
- [26]. Wang , Y., & Bian, N. (2015). Research of MPPT Control Method Based on PSO Algorithm. *Computer Science and Network Technology*, (pp. 698-701). Harbin,China.

- [27]. Batteries-Types & Working. (s.d.). Récupéré sur EL-PRO-CUS:
<https://www.elprocus.com/batteries-types-working/>
- [28]. Balog, R., & Davoudi, A. (2013). Batteries, Battery Management and Battery Charging Technology. Texas,USA.
- [29]. P.Manimekalai, R.Hanikumar, & S.Raghavan. (2013). An Overview of Batteriesfor Photovoltaic Systems. Computer Applications, 28-32.
- [30]. Emile, Y., Nabil, K., & Pamela, H. (2015). Review on different Charging Techniques of Lead-acid Batteries. Technological and Computer Engineering, (pp. 27-32). Koura,Lebanon.